An Analysis of Two - Layered Flows In Pipelines

A thesis presented in partial fulfillment of the requirements for the degree of

Master of Science
in
Mathematics

at Massey University, Albany,
New Zealand.

Bernard Ee

2003

Abstract

In this thesis, we consider the two-layered fluid flow problem in a circular pipeline. The justification of the model we shall employ, namely the stratified flow model will be discussed.

Our mathematical model is built from first principles, the conservation relations of mass, momentum and energy will be analysed and applied to the various flow configurations. We start by considering the simplest case possible, i.e. the planar axial interface and then extend the model by considering first, the motion of a travelling jump in the pipe section and second, to allow a small interfacial gradient.

The stability of the steady flow configuration is investigated using a linear stability method. This method starts off by assuming a travelling wave solution for the perturbation and then observing whether there is growth (unstable) or decay (stable) in this perturbed state. A stability map is provided to indicate the various possible scenarios for the travelling perturbation wave.

Acknowledgements

I would like to thank my supervisor, Professor Robert McKibbin for his patience, consistent encouragement and never-failing advice as I worked through the thesis material. In addition, I wish to express my appreciation to the staff and Mathematics postgraduate students at the Institute of Information and Mathematical Sciences for their administrative and moral support that they have extended to me over the course of the preparation of this thesis.

Table of Contents

Chapter 1

INTRODUCTION

1.1 General Survey & Literature Review

SANTOS Ltd is Australia's biggest supplier of natural gas. It operates nearly 600 wells, most of which are in South Australia. Generally, the wells produce a mixture of raw, dense gas with some water and a kerosene like condensate. These fluids pass through a compressor and are then pumped at high pressure through pipelines up to 180 km long to processing facilities. Both gas and liquid are carried in one pipe, but they travel at different speeds. In pipes across an undulating terrain such as those operated by SANTOS, a major cause of slugging, resulting in severe mechanical vibrations in the pipe, is the topography.

At the Mathematics-in-Industry Study Group (MISG) 2002 conference in Adelaide, South Australia, SANTOS had posed a challenge to develop a simple way to estimate peak liquid flow rates, slug sizes and the period between peaks. Although we are dealing with a liquid and a gas, we shall later prove that the best model to describe this problem presented by SANTOS was a liquid-liquid flow system. With this assumption, we shall go on to investigate the possible models allowed under such flow configurations, which will be detailed in this thesis. Now, we shall now provide a historical review of the development in liquid-liquid flow systems.

Co-flows of two immiscible liquids are encountered in a wide range of processes and equipment. In particular, oil-water flows have been of great commercial significance for some time. It was found that the introduction of a small amount of water in a long distance transport pipeline reduced the total frictional pressure drop along the pipeline and so decreased the amount of energy required to pump the oil; this was patented by Isaacs and Speed [1].

The accurate prediction of oil-water flow characteristics such as water hold-up, which may be used to determine the interfacial depth, and the average pressure gradient is important in numerous engineering contexts. However despite their importance, liquid-liquid flows have not been investigated to the same extent as gas-liquid flows. Essentially, a gas-liquid system is a two-fluid system characterized by low density and viscosity ratios. While there are many similarities between the gas-liquid and liquid-liquid systems, we cannot immediately apply the concepts of the former scenario to the latter because non-Newtonian behaviour is possible, notably for certain oils and oil-water emulsions.

Flow patterns as observed in liquid-liquid systems can be classified into four fundamental regimes:

a. Stratified flow with either smooth or wavy interface.

b. Large slugs, elongated or spherical, of one liquid in the other.

c. A dispersion of fine droplets of one liquid in the other. (the fluids are immiscible).

d. Annular flow where one fluid forms a flowing annulus and the other liquid flows in the core.

In many cases encountered, the resulting flow patterns are a combination of the above regimes (see Figure 1).

As in gas-liquid systems, the flow pattern observed depends on the separate liquid flow rates, physical characteristics (viscosity, surface tension and density), tube diameter and pipe section inclination. However if the density differential is relatively low, the role of gravity in liquid-liquid systems diminishes and the wall wetting and surface tension take on added significance in the resulting flow patterns. The liquids' wall-wetting is not just a property of the fluid material but also depends on the history and dynamics of the liquids near the wall surface [2-3]. Consequently, start-up procedures and entrance conditions may also affect the flow pattern. [4-6].

At this juncture, we shall conduct a brief survey of the various types of flow patterns, emphasizing stratified and core-annular flow patterns as the latter two are common for oil-water systems. While there are various ways to classify the various flow patterns discussed, the approach used in [7] will be adopted here. First, we need to define a certain non-dimensional constant called the Eötvos number, $E_{OD} = \frac{\Delta\rho g D^2}{8\sigma}$ where $\Delta\rho$ is the density difference between the liquids, g is the gravitational constant, D is the tube diameter and σ is the surface tension (assumed constant for prescribed fluids). The Eötvos number is the most important means of determining the appropriate model to use.

1.2 Stratified Flows

Stratified flow is defined as the basic flow pattern in horizontal or slightly inclined liquid-liquid systems with a finite density differential since it has been proven experimentally that, for low flow rates, the two liquid phases tend to segregate.

For liquid-liquid flows, it is not generally known whether which phase is travelling faster (subject to specified operational conditions). Multiple solutions can be obtained for the various operating environments in co-current (both fluids flowing in the same direction) and counter-current (both fluids in opposite directions) inclined flows. Furthermore, surface tension and wetting effects become relevant when there is a low relative density difference between the liquids.

As highlighted earlier, we can classify stratified flows according to the nature of the cross-sectional interface: smooth (plane, convex and concave) or wavy. It is assumed that the interface has a very small gradient along the axis of the pipe section, i.e. radius of curvature is still very large. If gravity is the dominant force in the system, then we will have a planar cross-sectional interface configuration. However, if surface effects (surface tension and wetting) are dominant, then the interfacial cross-sectional will attain a convex or concave configuration depending on the

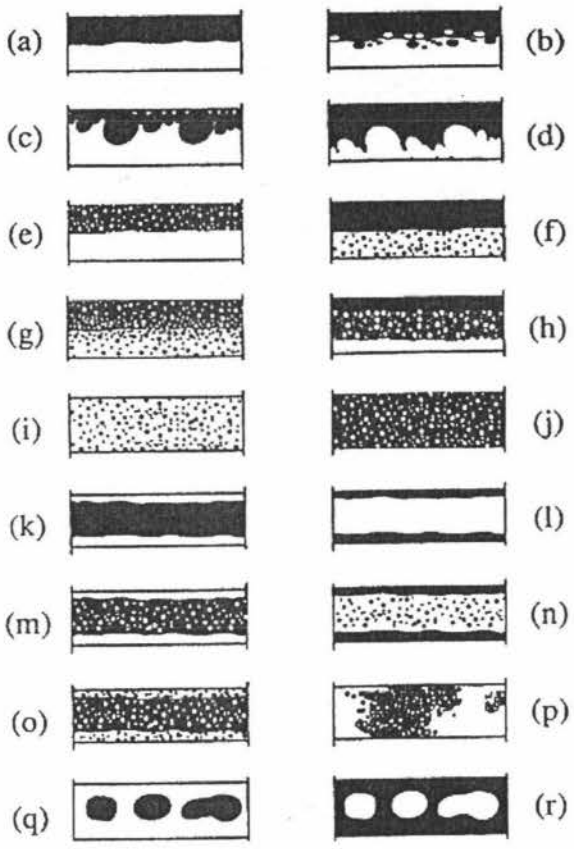

Figure 1 - Schematic of Possible Stratified Flow Patterns [7]

a/b Stratified flow model of two separated layers (with possible mixing at the interface)

c/d Stratified layers of a free liquid and dispersion of the other liquid (e.g. oil in water dispersion above a water layer)

e/f Stratified layers of a free liquid and dispersion of the other liquid (e.g. oil and oil-in-water dispersion)

g/h Layers of dispersion (e.g. water-in-oil-dispersion above oil in water dispersion, possibly with pure oil at the top and/or water at the bottom)

i/j Full dispersion or emulsion of one liquid in the other liquid. (e.g. water-in-oil or oil-in-water dispersion or emulsion)

k/l Core annular flow (e.g. a core of viscous oil and water in annulus)

m/n Annular flow of a liquid with dispersion in the core.

o Core annular flow of two dispersions.

p Intermittent flow (one liquid alternately occupying the pipe as a free liquid or as a dispersion.

q, r Long elongated or spherical bubbles of one liquid in the other.

relative wettability properties of the fluids and the wall surfaces [7]. Examples of this are shown in Figure 2.

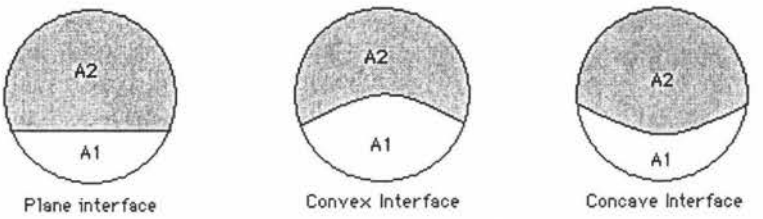

Figure 2 – A sketch of smooth cross-sectional interface configurations.

With increasing flow rates, the axial interface may be wavy, with possible entrainment (i.e. trapping through turbulence or chemical reaction) of drops above and/or below the interface [7]. Examples of this scenario are seen in Fig. 1b, e-g. As we shall later show, we will adopt the planar configuration model, allowing a possible and small interfacial variation along the axis of the pipe section. Such a model is known as the two-fluid model (TFM). According to [7], this is a useful model for practical applications and, as such, will be the model that we employ for the remainder of this thesis.

1.3 Annular Flows

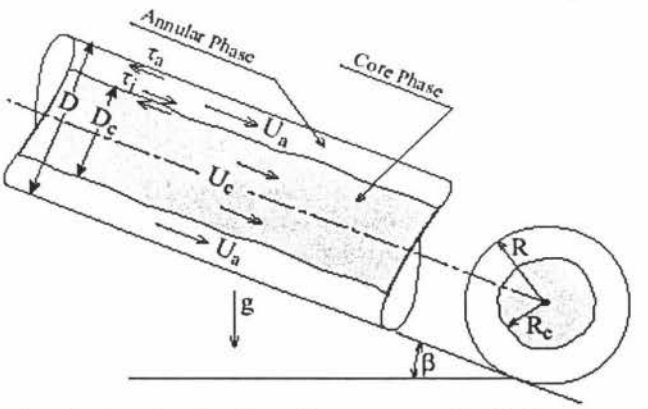

Figure 3 - Sketch of fully-developed Core Annular Flow flow pattern with β being the angle of inclination [7].

Under certain conditions, as given later in the section, it is possible for the oil and water to stabilise into a core (more viscous fluid) and annular (less viscous fluid) configuration. Such a flow scenario, shown schematically in Figure 3, is ideal as far as the minimisation of the applied pressure and flow energetics are concerned [7].

Numerous experiments done by Oliemans [8], Oliemans and Ooms [9] and Joseph and Renardy [10] proved that if a stable core flow can be maintained, then the pressure drop is almost independent of the oil viscosity and only slightly higher than for the flow of water alone at the mixture flow rate. To maintain such a flow pattern, the following need to be achieved:

a. Minimisation of the density differential between the oil (more viscous) and the water (less viscous fluid) by using additives and surface active agents for controlling and minimising the emulsification of water into oil.

b. Use of a hydrophilic pipe (strong affinity for water) pipe in order to prevent the oil phase from sticking to the wall.

c. Maintenance of a critical (minimum) oil superficial velocity and water/oil volume ratio to avoid contamination of the upper tube wall by the oil core. Below this critical oil superficial velocity, a transition to stratified flow regime will occur.

1.4 Stratified Flow Model & Analysis

As the SANTOS data (see table 1) supports the stratified flow model, we consider the case of stratified flows henceforth.

Table 1: SANTOS data presented at the MISG 2002

Quantity	Symbol	Value	Units
Lower Layer (denser liquid)			
volume flux	q_1	0.008	$m^3 s^{-1}$
density	ρ_1	550	$kg\,m^{-3}$
dynamic viscosity	ν_1	2.4×10^{-7}	$m^2 s^{-1}$
Upper Layer (lighter liquid)			
volume flux	q_2	0.4	$m^3 s^{-1}$
density	ρ_2	140	$kg\,m^{-3}$
dynamic viscosity	ν_2	1.3×10^{-7}	$m^2 s^{-1}$

Evidently, the best flow pattern that matches the flow parameters is that of the stratified flow model. This is because of the following:

i. Range of angle inclinations is very small from -1 to $+1$ degrees => slightly inclined system

ii. Relatively low flow rates for both liquids => two liquid phases will segregate.

iii. Density differential is high, i.e. $\Delta\rho/\rho_1 = 0.75 > 0.1$ => gravity dominant system

More critically, the planar interface configuration can be adopted as well since as shown in Figure 3. Furthermore according to [7], the core annular flow has been experimentally proven not to work in scenarios involving a high relative density differential, $\Delta\rho/\rho_1$ and a relatively low viscosity for the lighter liquid (upper layer).

In [7], the interface can be identified using the triple point (TP) and the interfacial curvature (Φ^*), as illustrated in Figure 4. Φ_0 is the between the vertical centre line and the line joining the centre-point to the triple point (TP), which is the contact points between the wall and the interface. Hence, different interfacial configurations (planar, convex and concave) will yield different TP locations and interfacial curvatures.

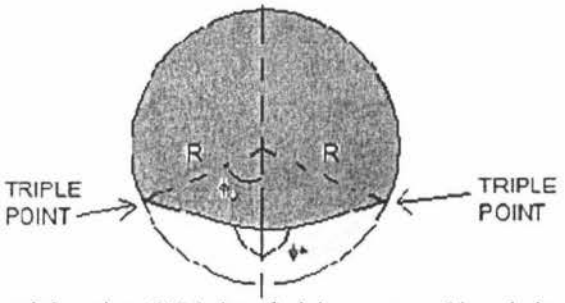

Figure 4 - A sketch of the triple points (TPs), interfacial curvature, Φ^* and phase distribution angle, Φ_0

The Interface Monograms, illustrated in Figure 5, show the relationship between the interfacial curvature and the phase distribution angle, while varying the contact angle between the interface and the wall, α (not the same as the angle of inclination) from 0 to π. Each point along an interface monogram is associated with a different hold-up (fraction of the flow area occupied by the lower, denser liquid layer). Together with the full solutions of the variables in the flow system (such as fluid layer speeds, interfacial height), we can also obtain the interfacial curvature.

In gravity dominated systems, we see that the planar configuration is a fair approximation as we see that for most Φ_0 values, the interfacial curvature is π, hence implying a planar interface. Furthermore, this also verifies the assumption that the liquid-gas flows can be approximated by a liquid-liquid system.

While we are not discarding surface tension effects here, we are asserting that gravity plays the dominant role in the flow configuration. In the coming chapters of this thesis, I shall then consider the scenario if we allow a slight variation in the interfacial gradient along the axis of the pipe section. This is particularly useful if we make transitions from one pipe section to another which will result, as we shall show, some form of interfacial height adjustment.

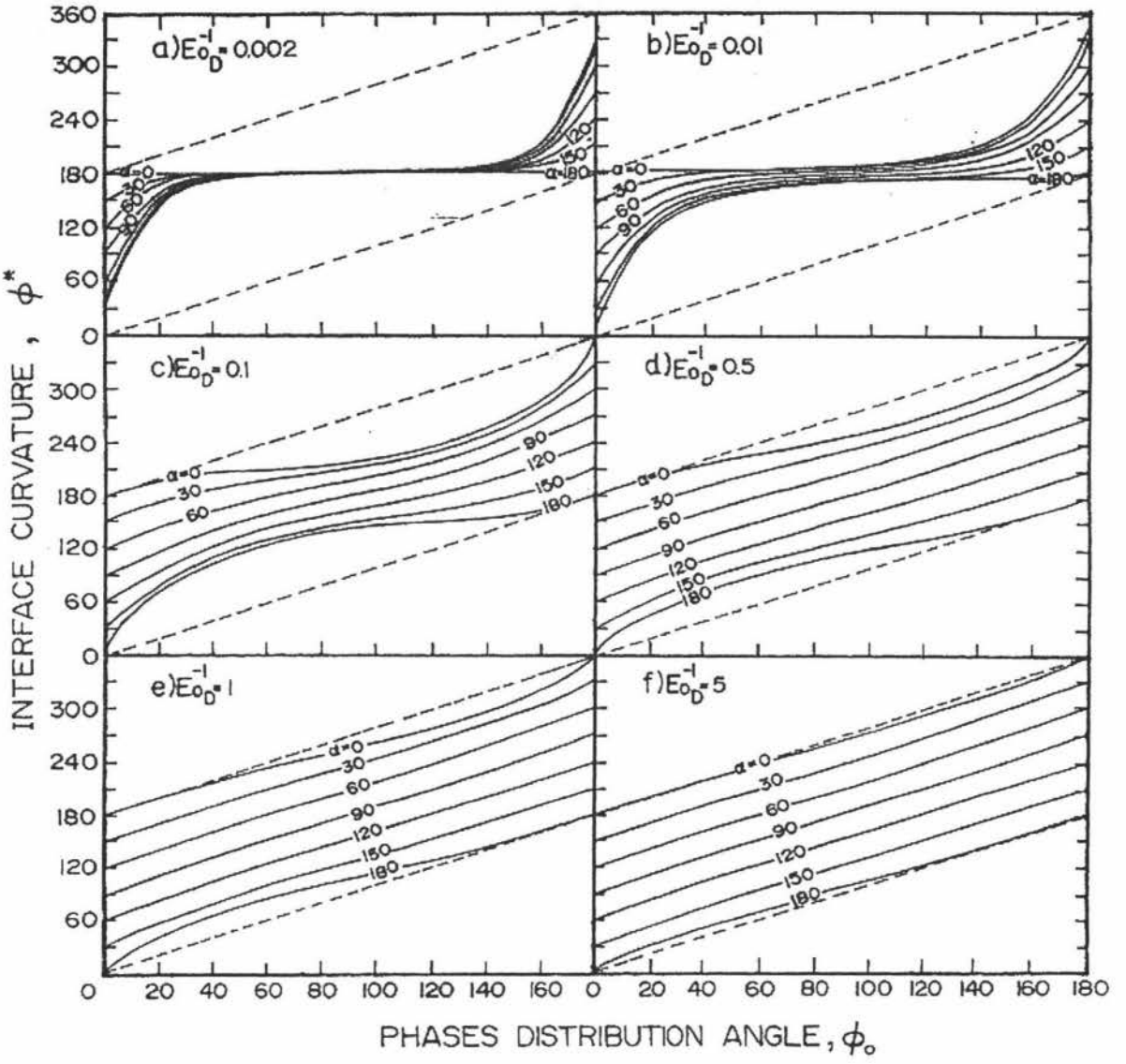

Figure 5 - Interface Monograms relating the interfacial curvature and the Eötvos number and contact angle, α between interface and wall [11]

1.5 Nomenclature

We need to define some of the terminology used here as well as highlight the derivations of the shear stresses that we will be using throughout this manuscript.

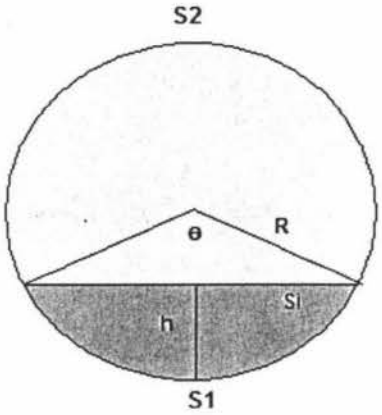

Figure 6 - A sketch of the cross section of the pipe

Table 2: Pipe parameters & Flow geometry:

Quantity	Symbol	Value/Function	Unit
Pipe parameters:			
Internal pipe radius	R	0.2	m
Internal cross sectional area	A_c	πR^2	m^2
Flow geometry parameters:			
Angle subtended by Interface	θ	$2\arccos\left(\frac{R-h}{R}\right)$	- (radians)
Interfacial width	S_i	$2\sqrt{2Rh-h^2}$	m
Wetted perimeter of liquid 1	S_1	$R\theta$	m
Wetted perimeter of liquid 2	S_2	$R(2\pi-\theta)$	m

At this juncture, we shall specify the assumptions employed in this scenario.

(1) Fluids are immiscible and incompressible.

(2) Fluid flow is steady (i.e. no time dependence)

(3) Pressures in fluids are assumed to be hydrostatic and so the relations are given as follows, where $P_0(z)$ is the pressure at the base of the pipe section.
$P_1 = P_0 - \rho_1 g y \cos(\alpha)$ & $P_2 = P_0 - \rho_1 g h \cos(\alpha) - \rho_2 g(y-h)\cos(\alpha)$

(4) Fluid system is stably stratified, i.e. $\rho_1 > \rho_2$

(5) Mass is conserved (i.e. no change of mass of fluid during the process)

(6) Thermal effects due to friction between liquids and the wall, and internal energy changes

in the liquids are neglected.

(7) Lower liquid layer is assumed to be an open channel flow while the upper liquid layer is a closed channel flow.

(8) Interfacial shear stress experienced by both liquids are assumed to be equal and opposite.

Shear forces that are at work are dependent on both the viscosity of the fluid and the roughness of the wall. The former is typically represented by the Reynolds number, whose formula for single phase pipe flow, is given below.

$$Re = \frac{\rho V D}{\mu} \tag{1.1}$$

where ρ is the density of the fluid, V is the average velocity, D is the diameter of the pipe, μ is the dynamic viscosity of the fluid medium.

Returning to our original flow problem involving two layered fluid system, the wetted perimeter for the lower layer is defined to be $S_1 = R\theta$, while $S_2 = (2\pi R\text{-}S_1) + S_i$, where S_i is the interfacial width, is the wetted perimeter for the upper layer. The reason for such a formulation is because we are assuming that the upper layer is lighter and hence dragging on the lower layer as the two fluids move in the axial direction. Hence, the upper fluid layer is assumed to be a closed channel flow and the lower fluid layer is an open channel flow. (see assumption (7) above).

So for our two-fluid problem, (1.1) can be modified as follows:

$$\mathrm{Re}_1 = \frac{u_1(4A_1)}{\nu_1 S_1} \tag{1.2a}$$

$$\mathrm{Re}_2 = \frac{u_2(4A_2)}{\nu_2 S_2} \tag{1.2b}$$

where u_1 and u_2 are the average fluid velocities for the layers, A_1 and A_2 are the cross sectional areas occupied by the liquids, S_1 and S_2 are the wetted perimeters of the liquid layers, the dynamic viscosities are defined as $\nu_k = \frac{\mu_k}{\rho_k}$ and the hydraulic diameter is defined to be $D_k = \frac{4A_k}{S_k}$ where k = 1, 2, is the index referring to the specified liquid layer.

Next, we need to consider the roughness of the pipe. Employing Knudsen and Katz's [12] smooth tube correlation rules, we have:

$$f_1 = \frac{0.046}{Re_1^{0.2}} \tag{1.3a}$$

$$f_2 = \frac{0.046}{Re_2^{0.2}} \tag{1.3b}$$

where f_1 and f_2 are friction factors, which describe the relationship between the fluid viscosity and pipe wall.

Applying single phase methods and Prandtl's mixing length formula, the wall shear stresses are characterised by the following relations:

$$\tau_1 = \frac{-f_1 u_1^2 \rho_1}{2} \tag{1.4a}$$

$$\tau_2 = \frac{-f_2 u_2^2 \rho_2}{2} \tag{1.4b}$$

We note that the shear stress terms: τ_1 and τ_2 are based on the assumption that the gradient of the interfacial height is very small and that the flows of the fluids are generally parallel to the axis of the pipe section.

Finally, we turn our attention to the interfacial shear stress terms. Gover and Aziz [12] proposed that the latter exists because the upper liquid layer dragging on the lower liquid layer, assuming that we have stable stratification. The friction factors are defined as,

$$\tau_{i1} = \frac{f_2 (u_2 - u_1)^2 \rho_2}{2} \tag{1.5a}$$

$$\tau_{i2} = \frac{f_2 (u_2 - u_1)^2 \rho_2}{-2} \tag{1.5b}$$

where f_2 is the friction factor for the lighter medium defined in (1.3b). Having done all these, we can now proceed with the core of this thesis.

1.6 Solution Methodology

In this thesis, we shall be making numerous references to the data given by SANTOS at the MISG 2002 meeting in Adelaide South Australia. As we have explained earlier in this introductory chapter, the model and assumptions employed here are unique to this particular flow data.

The primary goal of the thesis is to develop an understanding as to how the three fundamental relations, namely the conservation of mass, momentum and energy are applied to this flow scenario. It can be said that this model is applicable to scenarios with low flow rates and

large relative density differentials. After tackling the problem at its fundamental level, we can gradually increase the complexity of the flow scenario with the goal of building a coherent picture of the possible scenarios that can occur in a two-layered flow system in a circular pipe.

As such, the main purpose of this study is to gain an solid understanding of the mechanics of this flow scenario and to discover the limitations of the proposed model. Of course, it should be acknowledged that the material to be presented in this thesis builds on work done by other researchers, most notably, Fozard [13], Brauner [7,11,14] and the work undertaken by the MISG 2002 team, led by McGuinness and McKibbin [15].

Chapter 2

PLANE AXIAL INTERFACE PROBLEM

2.1 INTRODUCTION

Previously, we have shown that we can make the assumption that we have a planar configuration for the cross-sectional interface. In this chapter, we shall perform the analysis for the turbulent liquid-liquid flow problem with the assumption that $h(z)$ is a constant across a specified pipeline section, where $h(z)$ is the axial interfacial variation. This scenario represents the liquid-liquid problem at the most fundamental level and it is graphically represented as follows:

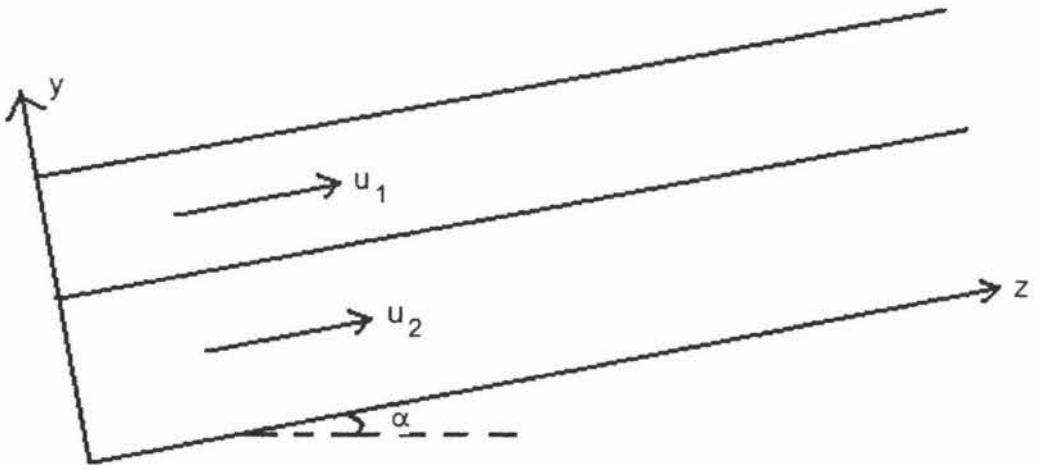

Figure 1a - Graphical description of Plane Axial interface problem where α is positive.

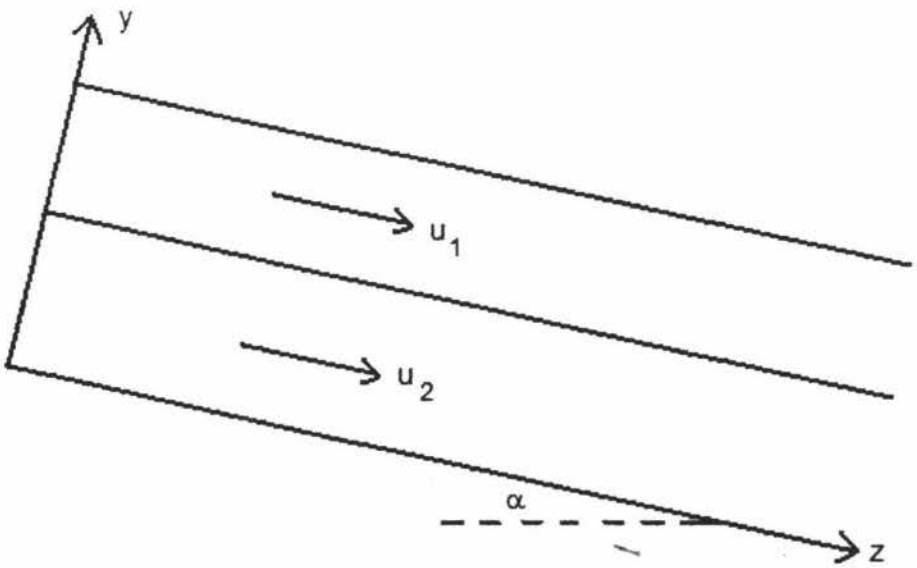

Figure 1a - Graphical description of Plane Axial interface problem where α is negative.

where we note that α is the angle of inclination of the pipe section. We shall define positive α when the pipeline is pointed upwards as shown in figure 1a. When the pipeline is pointed downwards, the α is then defined to have a negative value, shown in figure 1b. In addition, the two liquids have different average fluid velocities: u_1 and u_2, and the x-axis is directed into the page. We note that we are able to use average velocities as opposed to explicitly solving for the velocity is because of the interfacial approximation: very small gradients. In this analysis, we shall consider the following problems.

(1) How do we determine the uniform layer depth, h (depth of lower liquid 1) ?

(2) Is this uniform layer depth, h unique and in what way is this unique?

(3) What happens to h as α is negative or positive and how does the applied average pressure gradient, shear force terms change with each angle α ?

As we will be approaching the problem using first principles, we shall investigate the momentum and energy conservation relations using the calculus approach. In addition to the assumptions made in Chapter 1 (i.e. steady flows) and the introduction to this chapter, we are neglecting surface tension effects because the interface is parallel to the axis of the pipe section.

2.2 Problem Derivation & Solution Across Two Sections

Conservation of Mass: This principle allows us to obtain the average speeds of the two fluid layers. This is so because of the assumption that the interfacial slope is very small (i.e. close to horizontal), allowing us to make this approximation. So,

$$u_1 = \frac{q_1}{A_1} \tag{2.1a}$$

$$u_2 = \frac{q_2}{(A_c - A_1)} \tag{2.1b}$$

where A_1 is the cross-sectional area ratio occupied by the heavier lower fluid.

We first consider a slice of this pipe section of width $[z, z + \Delta z]$, the momentum conservation relation asserts that any changes of momentum flux in the slice is countered by the shear, gravitational forces and applied average pressure gradient which is mathematically expressed below.

$$\rho_k A_k u_k^2\Big|_z^{z+\Delta z} = \tau_k S_k \Delta z + (-1)^{k+1} \tau_i S_i \Delta z - \rho_k A_k \Delta z g \sin(\alpha) - \overline{P}_k A_k\Big|_z^{z+\Delta z} \tag{2.2}$$

where k = 1, 2 referring to the fluid layers as shown in figure 1 and $\overline{P}_k = \frac{1}{A_k} \int_{A_k} P_k dA_k$

is the average pressure function across the k^{th} fluid layer.

By setting $\Delta z \to 0$ and knowing that h is constant throughout the flow, the LHS of (2.2) is 0 leaving where each term is being evaluated at some point z^* in the interval $[z, z + \Delta z]$

$$0 = \tau_k S_k + (-1)^{k+1} \tau_i S_i - \rho_k A_k g \sin(\alpha) - \frac{d}{dz}\left(\overline{P}_k A_k\right) \tag{2.3}$$

Since A_k is a constant throughout the pipe section, we can extract it from the derivative operation. The condition for uniform flow is that the applied average pressure gradient across both equations are the same. In doing this, we obtain the following equation,

$$\frac{d\overline{P}_k}{dz} = \frac{\tau_1 S_1 + \tau_i S_i}{A_1} - \rho_1 g \sin(\alpha) = \frac{\tau_2 S_2 - \tau_i S_i}{A_2} - \rho_2 g \sin(\alpha) \tag{2.4}$$

for k = 1, 2 respectively where we note that the shear force and area functions are in terms of the interfacial height, h. So, solving (2.4) will yield the appropriate value of h. In this instance, I have used the matlab function 'fzero' to compute h. Using the matlab program (D:/Thesis Work / Chapter 2/main1.m), we obtain the following plots where we have used data from a MISG 2002 project (see Table 1 of Chapter 1).

A summary of the observations are given below.

(1) Negative and positive angles of inclination result in a shallowing and thickening of the interfacial height respectively. (see Figure 2a)

(2) At around $\alpha = -0.5$, the total shear forces per unit volume equals the gravitational force per unit volume implying that the average pressure gradient equals to 0 (see Figures 2a & 2b)

(3) At $\alpha = 0.465$ & 0.62, where the sum of shear forces per unit volume equals to 0, implying only gravity is at work. (see Figure 2b)

(4) The total shear force per unit volume is generally negative, except at $\alpha = 0.465$ & 0.62 where it is equals to 0 and α approximately between 0.465 and 0.62 degrees. (see Figure 2b)

(5) Average speed and Reynolds number for lighter fluid increases as the angle increases while it decreases for the heavier fluid. (see Figures 3 & 4)

(6) As the interfacial depth, h, increases, the kinetic energy flux per unit volume drops. This makes sense because the volume flux, i.e. q_1 and q_2 are preserved throughout the flow system, resulting in a decrease in average speeds. (see Figures 5a & 5b)

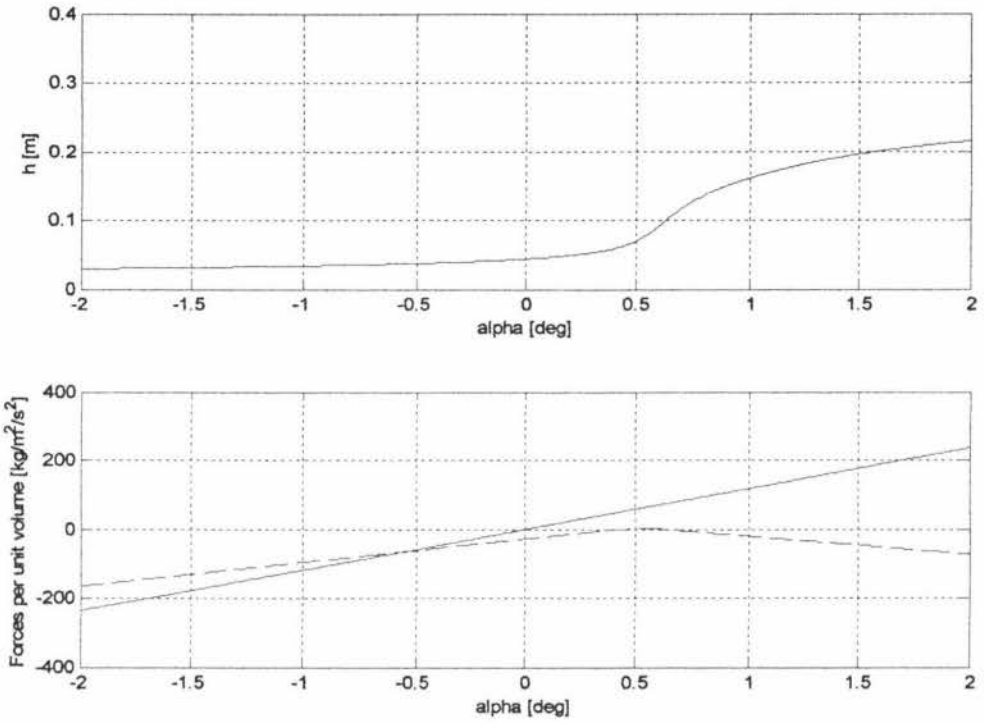

Figure 2a - Plots of interfacial height, h and forces (gravitational - bold and shear - dashed) per unit volume terms vs angle of inclination, α

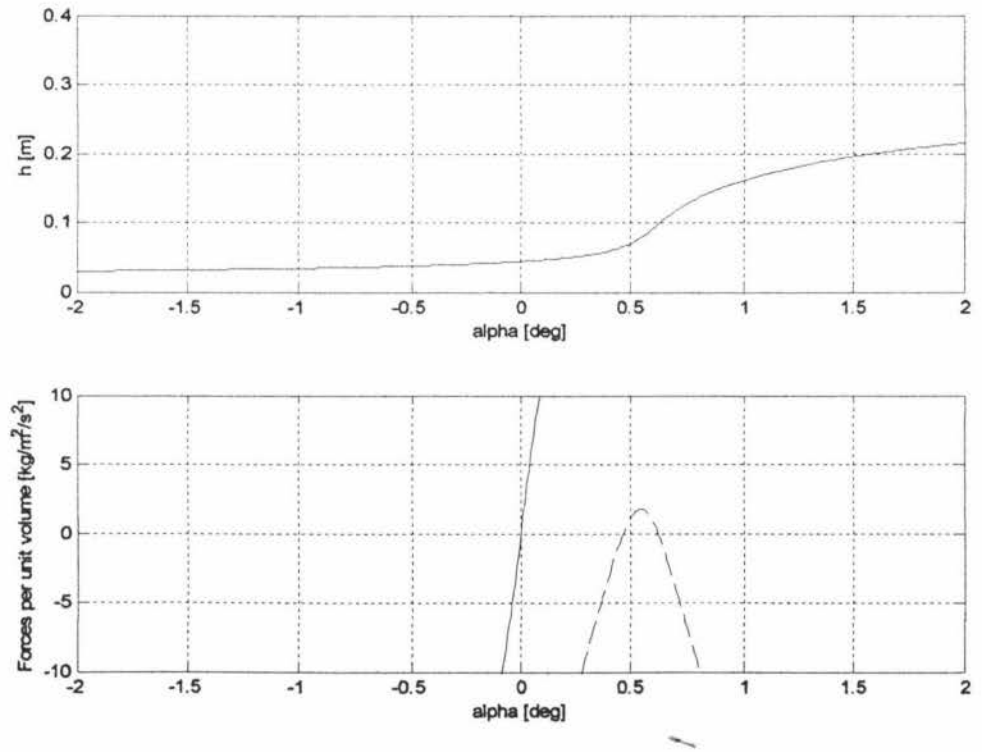

Figure 2b - Zoomed plots of interfacial height, h and forces (gravitational - bold and shear - dashed) per unit volume terms vs angle of inclination, α showing where the 2 force terms are equal

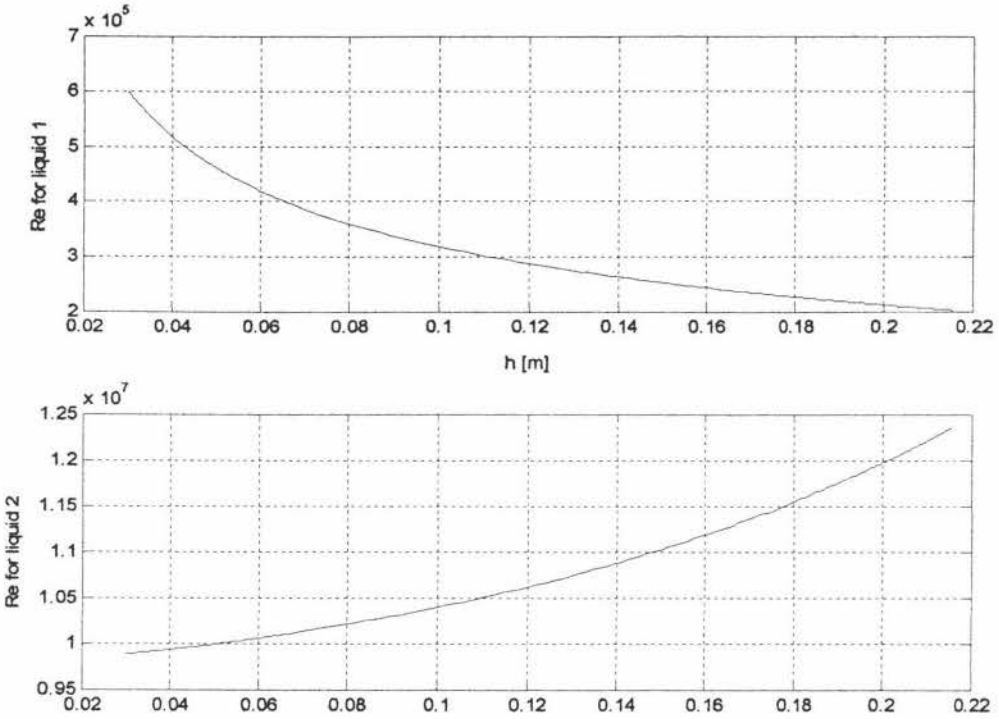

Figure 3 - Plots of Reynolds numbers for the two fluids vs interfacial height

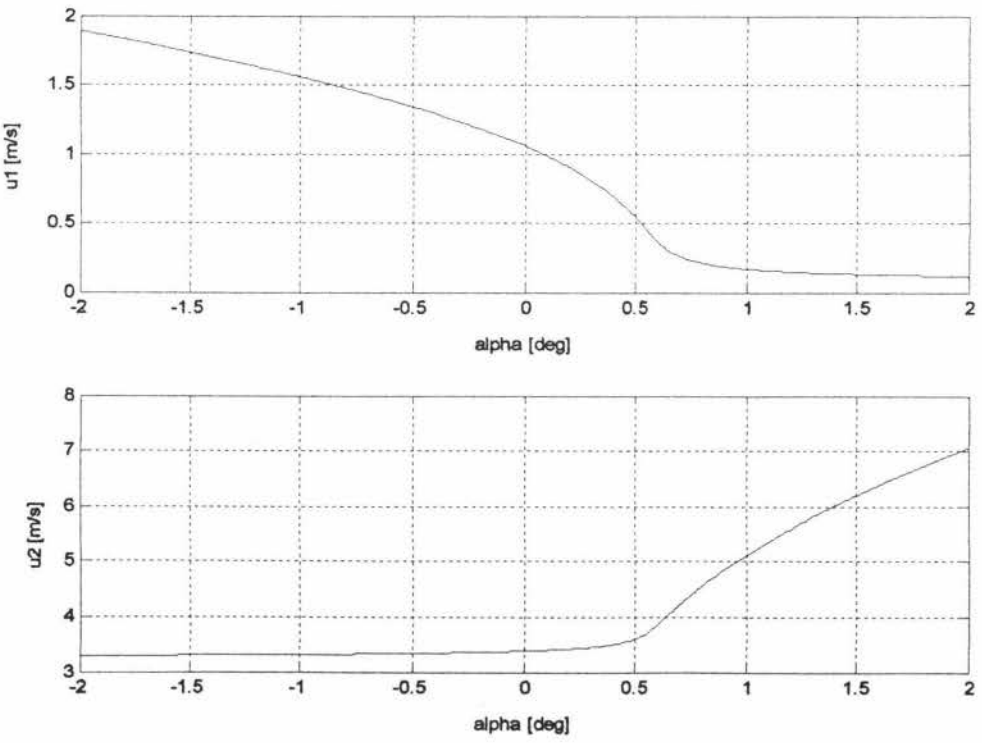

Figure 4 - Plots of Average fluid speeds vs angle of inclination, α

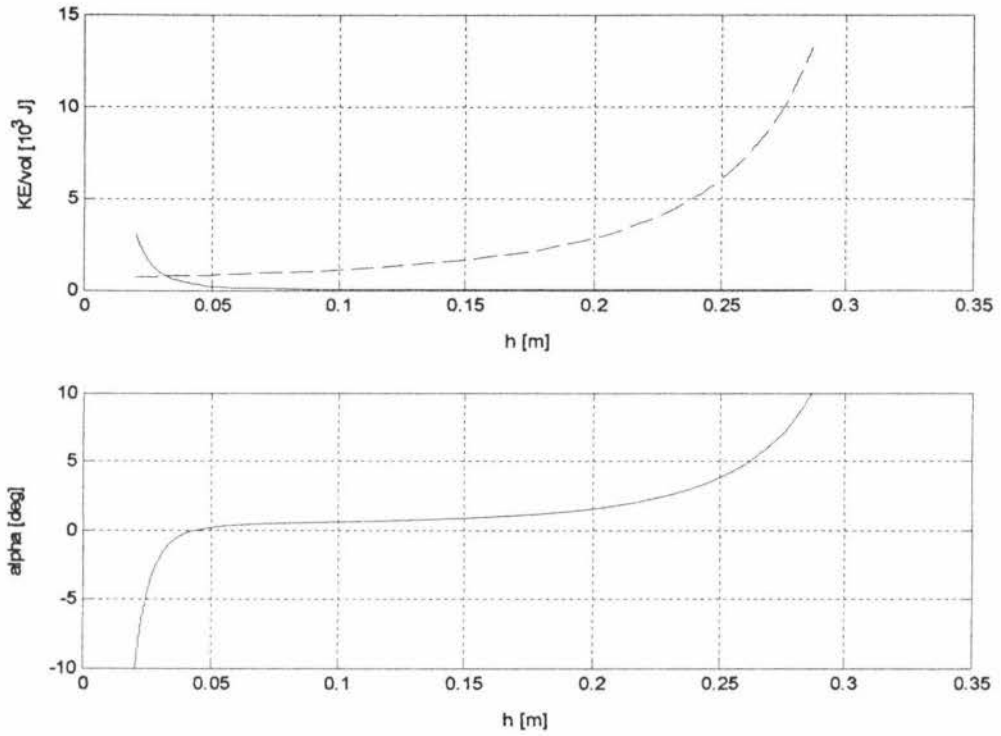

Figure 5a - Plots of kinetic energy flux and angle of inclination, α versus interfacial height (fluid 1 (heavier) - bold, fluid 2 (lighter) - dotted)

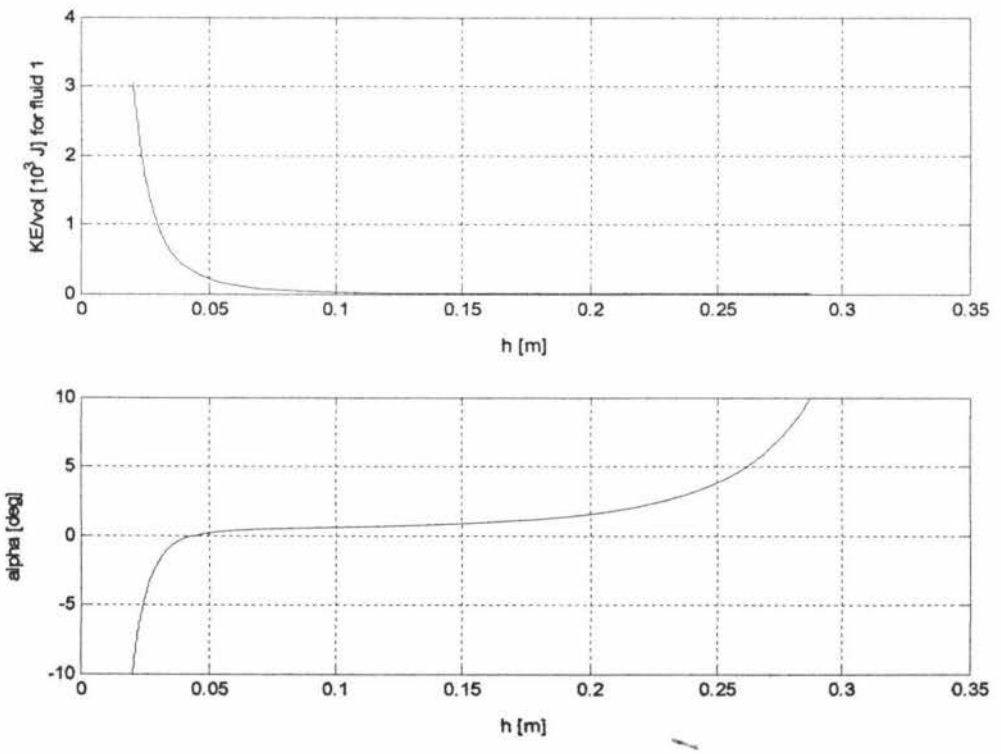

Figure 5b - Zoomed plots of kinetic energy flux and angle of inclination, α versus interfacial height

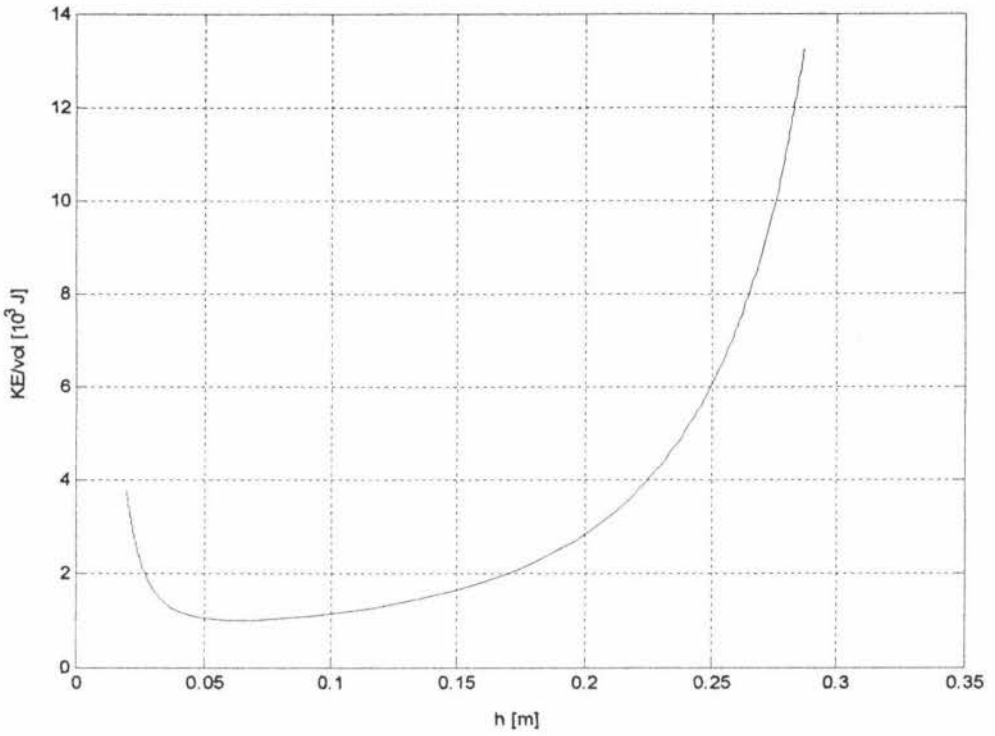

Figure 5c - Plot of total kinetic energy flux versus interfacial height

At this stage, the conditions in which (2.4) is not applicable should be noted. Clearly when either A_1 or A_2 equals 0 will we have a discrepancy, implying the existence of only one fluid as opposed to two. Of course, this doesn't mean that we will have an anomaly for such a scenario. Instead, it means that we need to deploy a single equation for a single fluid. For the latter case, the interfacial shear term is removed, set $\rho_1 = \rho_2$ and $A_1 = A_2 = \pi R^2$, we will then obtain the formula for average pressure gradient as follows:

$$\frac{d\overline{P}}{dz} = \frac{\tau_1 S_c}{A_1} - \rho_1 g \sin(\alpha) \tag{2.5}$$

where $S_c = 2\pi R$, the circumference of the pipe's cross section and we recall that this is for the steady case only.

We note that because the energy flux is constant along each pipe section with one angle of inclination, it is not useful to consider it. However as we will show in the next section, there will be a change of energy flux values because we will move from one pipe section to the next.

2.3 Energy & Momentum Considerations

Next, we shall complicate matters slightly by looking at the case where there is a sudden transition from one uniform flow regime to another, as shown in Figure 6, where α is negative

and α' is positive.

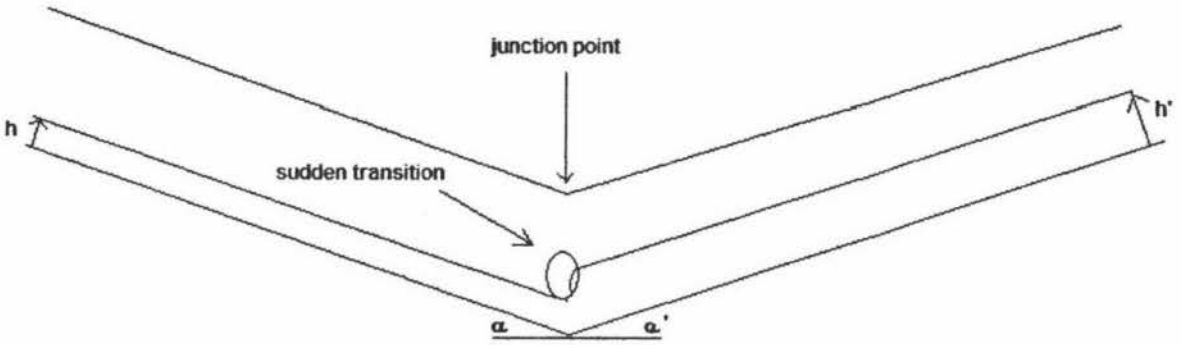

Figure 6 - Levelled Flow between 2 linked sections

This problem is a simplification of a case which will be discussed later in the long wave theory section. Essentially, we know that if there was a force induced at the junction point causing the interfacial height to jump from h to h'. For the above scenario, the critical considerations are the energy and momentum flux changes that are induced at the junction point. We first need to specify the assumptions that are employed in this problem.

(1) Transition region is small, relative to the size of the overall system.

(2) Average pressure gradients for both liquids are equal in each section.

(3) Volume fluxes are constant throughout each section.

(4) Forces balance in each section except possibly, at the pipeline junction.

Looking at the momentum flux relation first, we recall that any changes in the momentum flux across the transition must equal to the net force required to induce the change of momentum profile. First, the momentum flux term is defined as:

$$\text{momentum flux} = \frac{\text{momentum}}{\text{volume}} \text{ x volume flux}$$

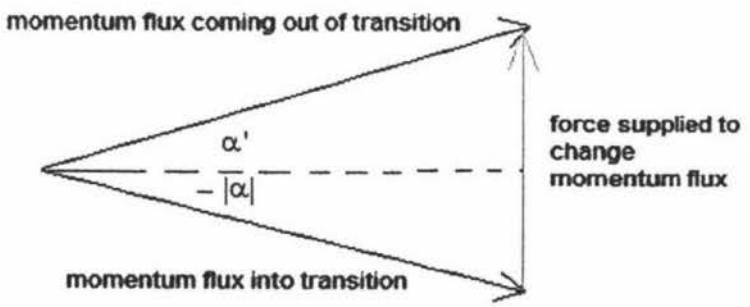

Figure 7 - a vector diagram to illustrate the momentum flux relation

Since we are looking at the forces (momentum flux terms), the latter terms have both magnitude and direction components as illustrated in the figure shown above. Using the simple cosine relation, we can determine what is the force that is required to change the momentum flux profile.

$$F^2 = (\rho_1 q_1 u_{1u} + \rho_2 q_2 u_{2u})^2 + (\rho_1 q_1 u_{1d} + \rho_2 q_2 u_{2d})^2 - 2(\rho_1 q_1 u_{1u} + \rho_2 q_2 u_{2u})(\rho_1 q_1 u_{1d} + \rho_2 q_2 u_{2d}) cos(\alpha' + |\alpha|) \quad (2.6)$$

where F is the force required to change the momentum profile, $(\rho_1 q_1 u_{1u} + \rho_2 q_2 u_{2u})$ and $(\rho_1 q_1 u_{1d} + \rho_2 q_2 u_{2d})$ are the momentum flux relations before and after the transition region respectively.

It should be noted that if α is negative, then the cosine term looks like $cos(|\alpha| + \alpha')$ or else it is $cos(\alpha' + \alpha)$, as usual. Furthermore, we see that if $u_{1u} = u_{1d}$ and $u_{2u} = u_{2d}$, then the angles are the same and the force supplied is subsequently equal to 0.

Turning our attention to the energy flux relation. We require that there will be an energy flux loss at the transition region because extra energy is required to change the momentum profile. If there is more than one junction in a pipeline network, we evaluate the energy flux losses based on two adjacent sections and not between the current section and first section (except for the first two).

The energy conservation principle states that any changes in the mechanical energy flux equals the net work rate of force in the pipe section. The energy flux is defined as:

$$\text{energy flux} = \frac{\text{energy}}{\text{volume}} \text{ x volume flux}$$

Mathematically, it is expressed as follows:

$$Q_e\Big|_z^{z+\Delta z} = [-g\,sin(\alpha)\rho_1 A_1 \Delta z - \tau_1 S_1 \Delta z + \tau_i S_i \Delta z]u_1 - \frac{d\overline{P}_1}{dz} u_1 \Delta z A_1 + [-g\,sin(\alpha)\rho_2 A_2 \Delta z - \tau_2 S_2 \Delta z - \tau_i S_i \Delta z]u_2 - \frac{d\overline{P}_2}{dz} u_2 \Delta z A_2 \quad (2.7)$$

where Q_e is the energy flux relation and all the functions above are evaluated at some point, say $z^* \in [z, z + \Delta z]$.

Now following the calculus approach and divide (2.7) by Δz and set $\Delta z \rightarrow 0$, we then obtain:

$$\frac{dQ_e}{dz} = \left[-g\sin(\alpha)\rho_1 A_1 - \tau_1 S_1 + \tau_i S_i\right]u_1 - \frac{d\overline{P}_1}{dz}u_1 A_1$$
$$+ \left[-g\sin(\alpha)\rho_2 A_2 - \tau_2 S_2 - \tau_i S_i\right]u_2 - \frac{d\overline{P}_2}{dz}u_2 A_2 \qquad (2.8)$$

The above equation gives us the energy flux differential for each pipe section. Since each of the terms in (2.8) are constant in z for each section, by our problem definition, we can generalise (2.8) to give the energy flux difference at the transition. Integrating (2.8) with respect to z and knowing that the energy flux profile is constant across each pipe section, we have:

$$\int_{z_\alpha}^{z_{\alpha'}} dQ_e = \int_{z_\alpha}^{z_{\alpha'}} \left\{\left[-g\sin(\alpha)\rho_1 A_1 - \tau_1 S_1 + \tau_i S_i\right]u_1 - \frac{d\overline{P}_1}{dz}u_1 A_1\right\} dz$$
$$+ \int_{z_\alpha}^{z_{\alpha'}} \left\{\left[-g\sin(\alpha)\rho_2 A_2 - \tau_2 S_2 - \tau_i S_i\right]u_2 - \frac{d\overline{P}_2}{dz}u_2 A_2\right\} dz \qquad (2.9)$$

where $z_{\alpha'}$ and z_α denote the axial points on the α' section and α section respectively.

The problem with the above approach is that we don't know the size of the transition region. In addition, the integrands for RHS in (2.9) are constant in each pipe section but it isn't the same constant in both pipe sections. So when we evaluate the integral, we will run into problems. Hence, we will adopt a simpler approach where the LHS of (2.8) is the difference between the total energy flux of the two fluid layers in the α section and α' section. This can be mathematically defined as follows:

$$Q_e\Big|_{z_\alpha}^{z_{\alpha'}} = \left[\frac{\rho_1 A_1 u_1^3}{2} + \frac{\rho_2 A_2 u_2^3}{2}\right]_{z_\alpha}^{z_{\alpha'}} \qquad (2.10)$$

2.4 Case Study

Now, we shall assume that we know the topography of the pipeline. In this case, we take $\alpha = sin(z)$ (see Figures 8a-c) and $\alpha = cos(z)$ (Figures 9a-c). The goal of this illustration is to apply the analysis that we have previously developed and try to reconcile, if need be, the data results with our theories. In addition, we need to add that the energy flux changes are determined by taking the difference in energy flux in two consecutive sections. In figure 8 shown below, we map the entire pipe section, pre-determined by our α function. We note that in this section, we are assuming that there is a sudden transition in interfacial depth from one section to another. Furthermore, the momentum flux change term represents the force exerted by the pipe on the fluids to change the momentum profile. Our observations are detailed below:

(1) Energy flux change is negative when α is decreasing, regardless of sign of α as we cross from one section to another => energy is lost when our angle decreases.

(2) At angular peaks, i.e. at $\alpha = -1$ and $+1$, the energy flux change is 0.

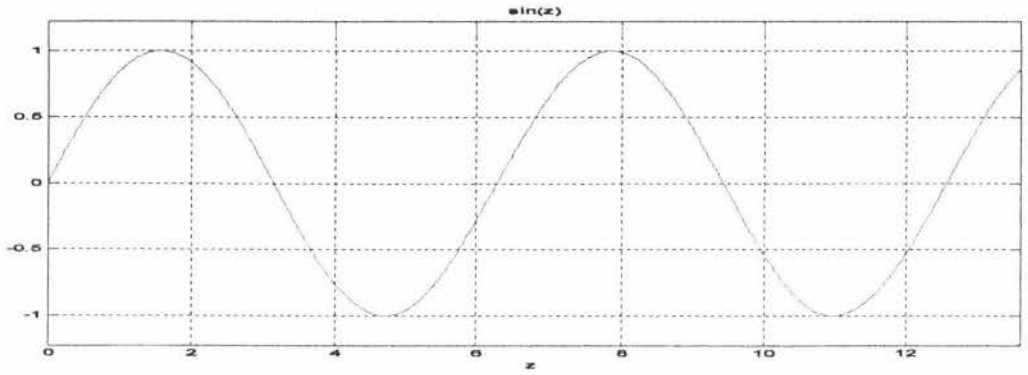

Figure 8a - A plot of the angular variation along the axis of the pipeline: *sin*(*z*)

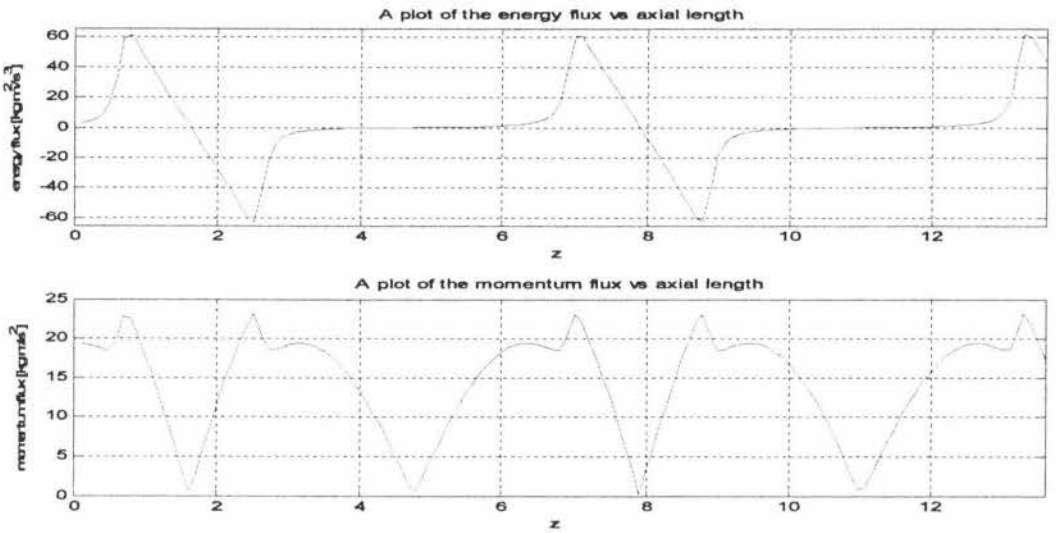

Figure 8b - Plots detailing the energy and momentum flux changes along the pipeline for *sin*(*z*)

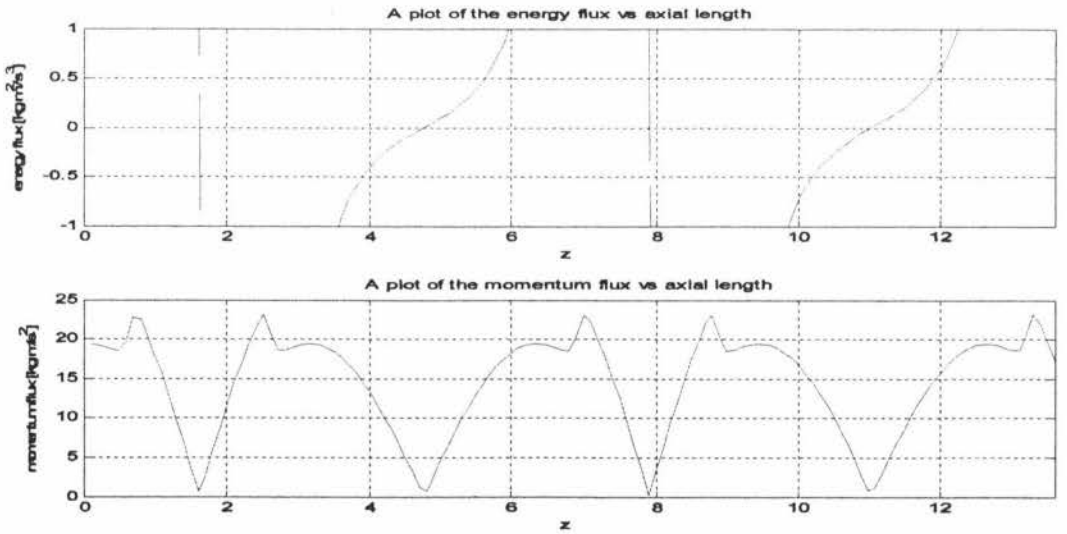

Figure 8c - Zoomed plots detailing the energy and momentum flux changes along the pipeline for *sin*(*z*)

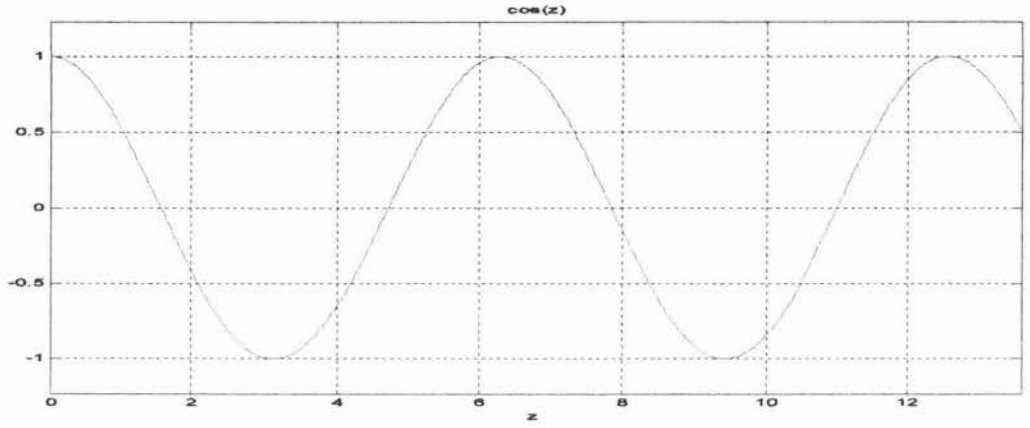

Figure 9a - A plot of the angular variation along the axis of the pipeline: *cos(z)*

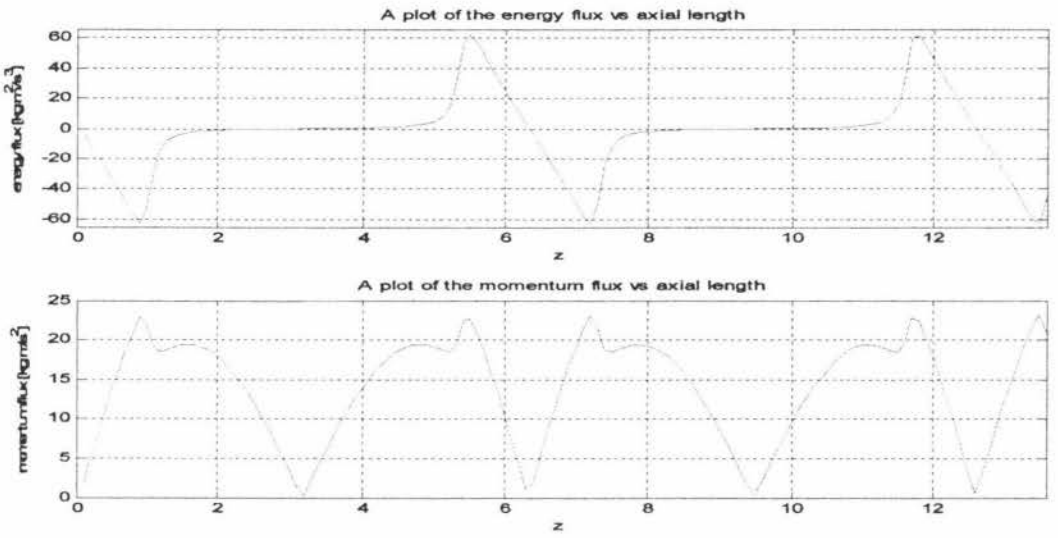

Figure 9b - Plots detailing the energy and momentum flux changes along the pipeline for *cos(z)*

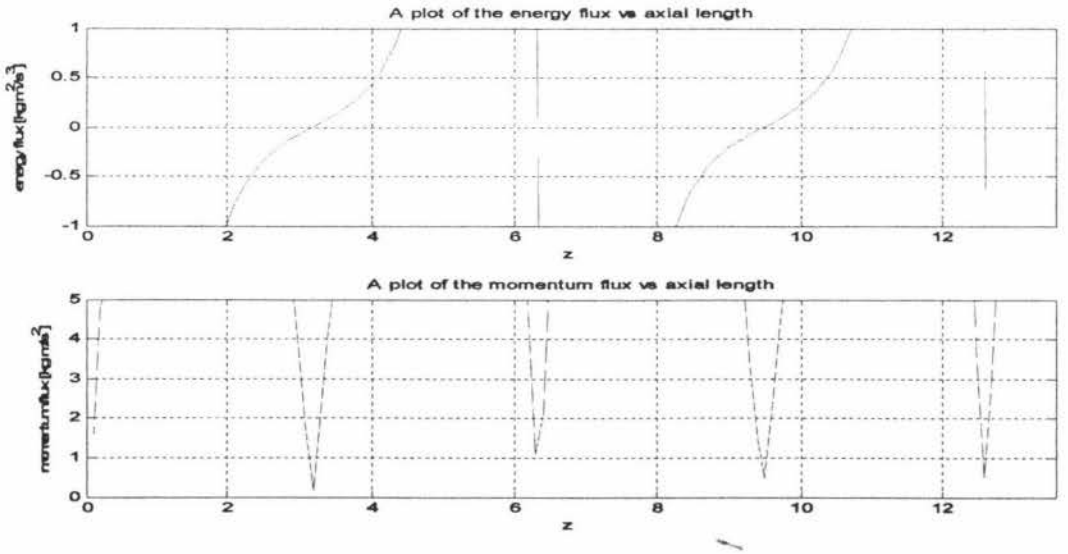

Figure 9c - Zoomed plots detailing the energy and momentum flux changes along the pipeline for *cos(z)*

(3) Energy flux change is positive when α is increasing, regardless of sign of α => energy needs to be added when the angle is increasing.

(4) Momentum flux change is minimal at angular peaks, i.e. at $\alpha = -1$ and $+1$. This means that when the original angle is -1 and $+1$, the resulting momentum flux loss is at a minima.

(5) Energy flux change peaks (absolute maxima and minima) correspond to maximum losses of momentum flux.

2.5 Closing Remarks

In this chapter, we considered the planar axial interface problem. This scenario constitutes the most fundamental description of our two-layered problem. Despite the apparent simplification of the problem, we are faced with numerous parameters like the angle of inclination, interfacial height, volume fluxes of the two liquids. As such, it was difficult to obtain an analytical form for the relationship between the interfacial height and the angle of inclination. Hence, a numerical approach was adopted.

In addition, we also described the analysis involving two connecting pipe sections, as illustrated in Section 2.3. Given that we are not able to characterise the transition region, i.e. the region at the junction point (see figure 6) and that the energy flux in each section of the pipe network is constant, the energy flux loss is described in terms of the energy flux difference between the two sections.

Chapter 3

TRAVELLING JUMP SCENARIO

3.1 Introduction

In this chapter, we shall consider the case where we have a travelling wave, jump or pulse inside a single pipe section, followed by a survey of conceptual models for the multi-section problem. We shall make the following assumptions used in this problem.

(1) Travelling wave/jump in this section has short wavelength, compared to overall length of the system, so that in the jump region, the wall shear and gravitational forces are dominated by the pressure and interfacial shear forces.

(2) Travelling wave/jump has a constant speed, V, which will be determined later as part of the solution process.

(3) Uniform flow regimes before and after the transition, i.e. in the latter conditions, the interfacial heights are constant in region before and after the jump.

(4) Fluids are moving close to parallel to the axis of the pipe section, which will allow us to take the average speed as defined in the introduction.

(5) Surface tension effects are neglected because of the smallness of the jump zone in question.

Sketches of this problem are given in Figure 1a.

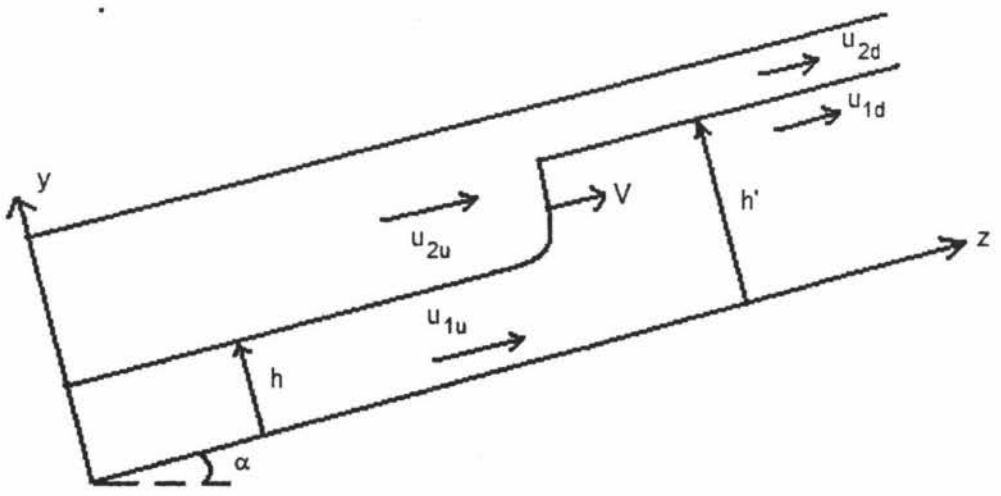

Figure 1a - Actual travelling wave scenario

If we consider this problem on a moving reference frame, i.e. to view the scenario from the point of view of the travelling wave itself, we can then take the relative motion of the fluids and the pipeline to the travelling wave (see Figure 1b). We note that we shall assume that the speed of the travelling wave is constant so as to give us an inertial reference frame as opposed to an accelerating reference frame which is of course more complicated. In both figures 1a and 1b, we shall denote the fluid layer speeds before the wave as u_{1u} and u_{2u} (where the subscript u refers to upstream) and after the wave as u_{1d} and u_{2d} (where the subscript d refers to downstream).

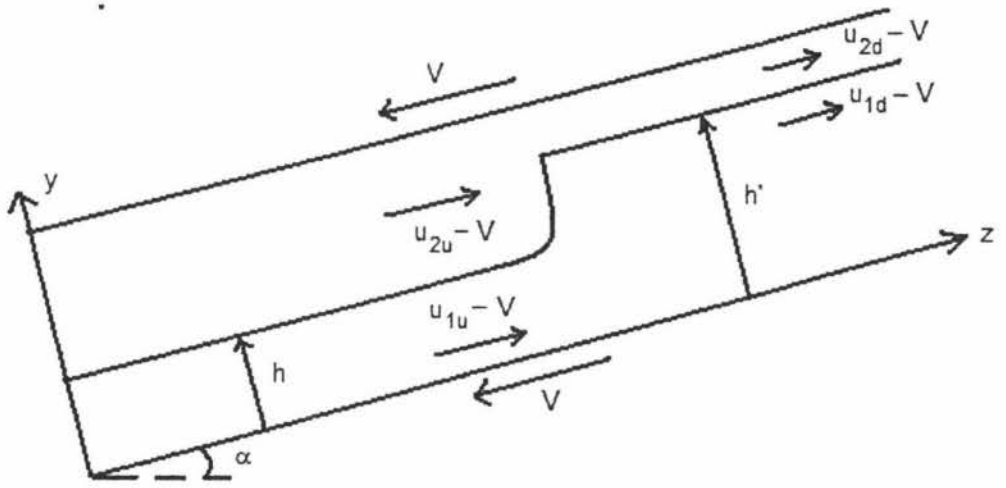

Figure 1b - A graphical representation of the relative stationary travelling wave problem

Tackling this problem from first principles, we shall look at each of the conservation principles: mass, momentum and energy.

3.2 Derivation of Equations

First, we consider the Conservation of Mass:

$$\rho_k A_{ku} (u_{ku} - V) = \rho_k A_{kd} (u_{kd} - V) \tag{3.1}$$

for k = 1, 2, referring to the liquid layer. If we are given the upstream speeds, we shall re-write (3.1) in terms of u_{kd} (downstream speeds) and obtain (3.2):

$$u_{kd} = V + \frac{A_{ku}}{A_{kd}} (u_{ku} - V) \tag{3.2}$$

In this problem, we will preserve the form of (3.2) until the end and then apply the average speed definition (2.1a and 2.1b) for the downstream regime.

Turning our attention to the Conservation of Momentum, we need to take into account all the forces at work. As stated earlier, we shall look at the interfacial shear, pressure forces and momentum flux changes since they are the dominant forces in the jump zone.

(i) Interfacial shear forces are applicable if we consider the forces at work on an individual basis but they are both equal and opposite on both liquids, say F for liquid 1 and $-F$ for liquid 2.

(ii) Since this is uniform flow, the average pressure gradient for both liquids are identical. If the jump zone is defined in $[z_1, z_2]$, then the total pressure force across each regime (upstream and downstream) is given by,

$$\int_{h}^{(2R)}\int_{z_1}^{z_2} \frac{d}{dz}\left(P_0 - \rho_1 g h\cos(\alpha) - \rho_2 g(y-h)\cos(\alpha)\right)S_i(y)\ dz dy \ + \int_{0}^{h}\int_{z_1}^{z_2} \frac{d}{dz}\left(P_0 - \rho_1 g y\cos(\alpha)\right)S_i(y)\ dz dy$$

where h is the interfacial height and $S_i(y)$ is the interfacial width. P_0 is the pressure at the base of the pipe ($y = 0$) and the hydrostatic pressure for liquid 1 and 2 are defined by $P_0 - \rho_1 g y\cos(\alpha)$ and $P_0 - \rho_1 g h\cos(\alpha) - \rho_2 g(y-h)\cos(\alpha)$ respectively.

(iii) By assumption (1) given earlier in this chapter, we can neglect the pipe resistance and fluids' body forces.

So, the momentum conservation relation states that any changes in the momentum flux equals to the net forces at work. (3.3a) and (3.3b) are the momentum balance equations for liquid 1 and liquid 2 respectively.

$$\rho_1 A_{1d}(u_{1d} - V)^2 - \rho_1 A_{1u}(u_{1u} - V)^2 = F + \int_0^{h_1'} 2\left(P_0 - \rho_1 g y\cos(\alpha)\right)\sqrt{R^2 - (R-y)^2}\ dy - \int_0^{h_1} 2\left(P_0 - \rho_1 g y\cos(\alpha)\right)\sqrt{R^2 - (R-y)^2}\ dy \quad (3.3a)$$

$$\rho_2 A_{2d}(u_{2d} - V)^2 - \rho_2 A_{2u}(u_{2u} - V)^2 = -F + \int_{h_1'}^{2R} 2\left(P_0 - \rho_1 g h_1'\cos\alpha - \rho_2 g(y-h_1')\cos(\alpha)\right)\sqrt{R^2 - (R-y)^2}\ dy - \int_{h_1}^{2R} 2\left(P_0 - \rho_1 g h_1\cos\alpha - \rho_2 g(y-h_1)\cos(\alpha)\right)\sqrt{R^2 - (R-y)^2}\ dy \quad (3.3b)$$

Now, adding (3.3a) and (3.3b) together, the interfacial force terms can be eliminated and hence

we obtain.

$$\rho_2 A_{2d}(u_{2d}-V)^2 - \rho_2 A_{2u}(u_{2u}-V)^2 + \rho_1 A_{1d}(u_{1d}-V)^2 - \rho_1 A_{1u}(u_{1u}-V)^2$$

$$= \int_{h_1'}^{2R} 2(P_0 - \rho_1 g h_1' \cos\alpha - \rho_2 g(y-h_1')\cos(\alpha))\sqrt{R^2-(R-y)^2}\ dy -$$

$$\int_{h_1}^{2R} 2(P_0 - \rho_1 g h_1 \cos\alpha - \rho_2 g(y-h_1)\cos(\alpha))\sqrt{R^2-(R-y)^2}\ dy +$$

$$\int_{0}^{h_1'} 2(P_0 - \rho_1 g y \cos(\alpha))\sqrt{R^2-(R-y)^2}\ dy -$$

$$\int_{0}^{h_1} 2(P_0 - \rho_1 g y \cos(\alpha))\sqrt{R^2-(R-y)^2}\ dy \qquad (3.4)$$

As we can see, (3.4) is a quadratic expression in V. However, we seek to simplify the RHS of (3.4) so as to be able to describe the properties and characteristics of certain components of our equation and how they behave under various angles of inclination.

It is evident that there are essentially two types of integrals which we can simplify, where $h = h_1'$ and h_1 refer to downstream and upstream depths respectively. They are given below. However, we shall consider the h_1 case and subsequently make the substitution for the h_1' case.

The first key integral is given below.

$$\int_0^{h_1} \left(2P_0\sqrt{R^2-(R-y)^2} - 2\rho_1 g\cos(\alpha) y\sqrt{R^2-(R-y)^2}\right) dy$$

$$= P_0 A_{1u} - \rho_1 g\cos(\alpha)\int_0^{h_1} \left(2y\sqrt{R^2-(R-y)^2}\right) dy$$

$$= P_o A_{1u} + \rho_1 g\cos(\alpha)\left\{\frac{2(2Rh_1 - h_1^{\,2})^{\frac{3}{2}}}{3} - RA_{1u}\right\} \qquad (3.5a)$$

Now, we look at the 2nd integral and following the same techniques of solving the integrals, we obtain.

$$\int_{h_1}^{2R} 2(P_0 - \rho_1 g h_1 \cos\alpha - \rho_2 g(y-h_1)\cos(\alpha))\sqrt{R^2-(R-y)^2}\ dy$$

$$= P_0 A_{2u} - (\rho_1-\rho_2) h_1 g\cos(\alpha) A_{2u} - \int_{h_1}^{2R} 2\rho_2 g y\cos(\alpha)\sqrt{R^2-(R-y)^2}\ dy$$

$$= P_0 A_{2u} - (\rho_1 - \rho_2) h_1 g \cos(\alpha) A_{2u} + \rho_2 g \cos(\alpha) \left(\frac{-2\left(2Rh_1 - h_1^2\right)^{\frac{3}{2}}}{3} - RA_{2u} \right) \quad (3.5b)$$

Then, we proceed to substitute (3.5a) and (3.5b) and the equivalent expressions for the downstream height, h_1' into (3.4). Subsequently, we shall make use of (3.2) to replace the downstream momentum flux expressions with the equivalent upstream expressions. Finally, we obtain the expression below.

$$\frac{2g\cos(\alpha)}{3}(\rho_1 - \rho_2)\left[\left(2Rh_1' - h_1'^2\right)^{\frac{3}{2}} - \left(2Rh_1 - h_1^2\right)^{\frac{3}{2}}\right] +$$
$$g\cos(\alpha)\left[R(A_{1u} - A_{1d}) + h_1 A_{2u} - h_1' A_{2d}\right](\rho_1 - \rho_2) +$$
$$\rho_1 A_{1u}(u_{1u} - V)^2\left(\frac{A_{1u} - A_{1d}}{A_{1d}}\right) + \rho_2 A_{2u}(u_{2u} - V)^2\left(\frac{A_{1d} - A_{1u}}{A_c - A_{1d}}\right) = 0 \quad (3.6)$$

where $A_{1d} = A_c - A_{2d}$ and $A_{1u} = A_c - A_{2u}$ where A_c is the cross sectional area of the pipe.

As we can see, (3.6) is a quadratic expression in V and the next step is to solve (3.6) for V and so obtain

$$V_1 = \frac{-b + \sqrt{b^2 - 4ac}}{2a} \quad ; \quad V_2 = \frac{-b - \sqrt{b^2 - 4ac}}{2a}$$

where the terms of V_1 and V_2 are given as

$$a = \rho_1 A_{1u}\left(\frac{A_{1u} - A_{1d}}{A_{1d}}\right) + \rho_2 A_{2u}\left(\frac{A_{1d} - A_{1u}}{A_c - A_{1d}}\right)$$
$$b = -2u_{1u}\rho_1 A_{1u}\left(\frac{A_{1u} - A_{1d}}{A_{1d}}\right) - 2u_{2u}\rho_2 A_{2u}\left(\frac{A_{1d} - A_{1u}}{A_c - A_{1d}}\right)$$
$$c = \rho_1 A_{1u}\left(\frac{A_{1u} - A_{1d}}{A_{1d}}\right)u_{1u}^2 + \rho_2 A_{2u}\left(\frac{A_{1d} - A_{1u}}{A_c - A_{1d}}\right)u_{2u}^2$$
$$+ \frac{2g\cos\alpha}{3}\cdot(\rho_1 - \rho_2)\cdot\left[\left(2Rh_1' - h_1'^2\right)^{\frac{3}{2}} - \left(2Rh_1 - h_1^2\right)^{\frac{3}{2}}\right]$$
$$+ g\cos\alpha\cdot\left[R(A_{1u} - A_{1d}) + h_1 A_{2u} - h_1' A_{2d}\right]\cdot(\rho_1 - \rho_2)$$

Having obtained our values of V, we can proceed to find the actual downstream height values noting that at this stage, we have yet to settle on a specific value of V.

3.3 Solution Process and Analysis

As we assume uniform flow conditions downstream (ahead of the travelling wave), we solve for the average pressure gradient term in the momentum equation in each fluid layer and then equalize (3.7a), for liquid 1 and (3.7b) and liquid 2, to obtain (3.7c):

$$\frac{d\overline{P}_{1d}}{dz} = \frac{\tau_{1d}S_{1d} + \tau_{id}S_{id}}{A_{1d}} - \rho_1 g\, sin(\alpha) \qquad (3.7a)$$

$$\frac{d\overline{P}_{2d}}{dz} = \frac{\tau_{2d}S_{2d} - \tau_{id}S_{id}}{A_{2d}} - \rho_2 g\, sin(\alpha) \qquad (3.7b)$$

$$\frac{\tau_{2d}S_{2d} - \tau_{id}S_{id}}{A_{2d}} - \rho_2 g\, sin(\alpha) - \left(\frac{\tau_{1d}S_{1d} + \tau_{id}S_{id}}{A_{1d}} - \rho_1 g\, sin(\alpha)\right) = 0 \qquad (3.7c)$$

noting that the shear and cross-sectional area terms are functions of the downstream height, h_1'. The solution process is outlined below (see MATLAB programme D:/Thesis Work/Chapter 3/main1.m).

i. Substitute test values of h_1' from a possible range of values in the interval (0, 2R), and the corresponding values of V_1 and V_2, using the test values of h_1', into the equation (3.7c). So, we will have two sets of values for the LHS of (3.7c).

ii. Take the absolute difference in the values of the LHS of (3.7c) and isolate the smallest difference for each set, corresponding to V_1 and V_2.

iii. Mark out the h_1' value which corresponds to this smallest absolute difference value of the LHS of (3.7c). This will be the approximation to 0 (RHS of 3.7c).

iv. Once that particular h_1' is identified, we check to see if this is equal to h_1. If yes, then set $V = 0$ and end the solution process.

v. If no, then proceed to check the energy flux loss criterion. If $Q_e < 0$, then it is the correct h value. Note that we will have different h_1' values for different V but they are uniquely determined.

It should noted that we are varying α from - 1 to + 1 degrees and see whether we will have a downstream height, h_1' and what would be the corresponding wave speed, V.

We can make the following observations about the plots above, noting that our total energy flux loss is defined as: $\left[\frac{1}{2}\rho_1 A_1 u_1^3 + \frac{1}{2}\rho_2 A_2 u_2^3\right]_{z_1}^{z_2}$ where $[z_1, z_2]$ is the axial length of the jump zone (where the travelling wave is located) and $z_1 < z_2$. We shall justify such a definition of the energy flux loss later in this chapter.

(i) Downstream heights, h_1' not very much different from h_1, where the latter, the upstream depth, is identified by the bold line (see 3rd plot of Figure 3). This difference in the interfacial heights is of the order of 0.1 cm. For $\alpha < 0.5$ degrees, there is no visible difference in downstream and upstream heights but there is a small but distinct difference for $0.5 \leq \alpha \leq 1$ degrees, giving rise to non-zero interfacial wave speeds in the latter α range.

(ii) V_1 results in energy flux loss while V_2 results in energy flux gain as we cross the travelling wave. Hence, V_1 values are the ideal wave speed values.

(iii) All Vs are positive in this range of given α values, implying that any possible travelling wave is moving in the direction of positive z.

(iv) α from + 0.5 degrees onwards results in distinctly different V values. Prior to that, all our $h_1 = h_1'$, which implies that we have no travelling wave and $V_1 = V_2 = 0$.

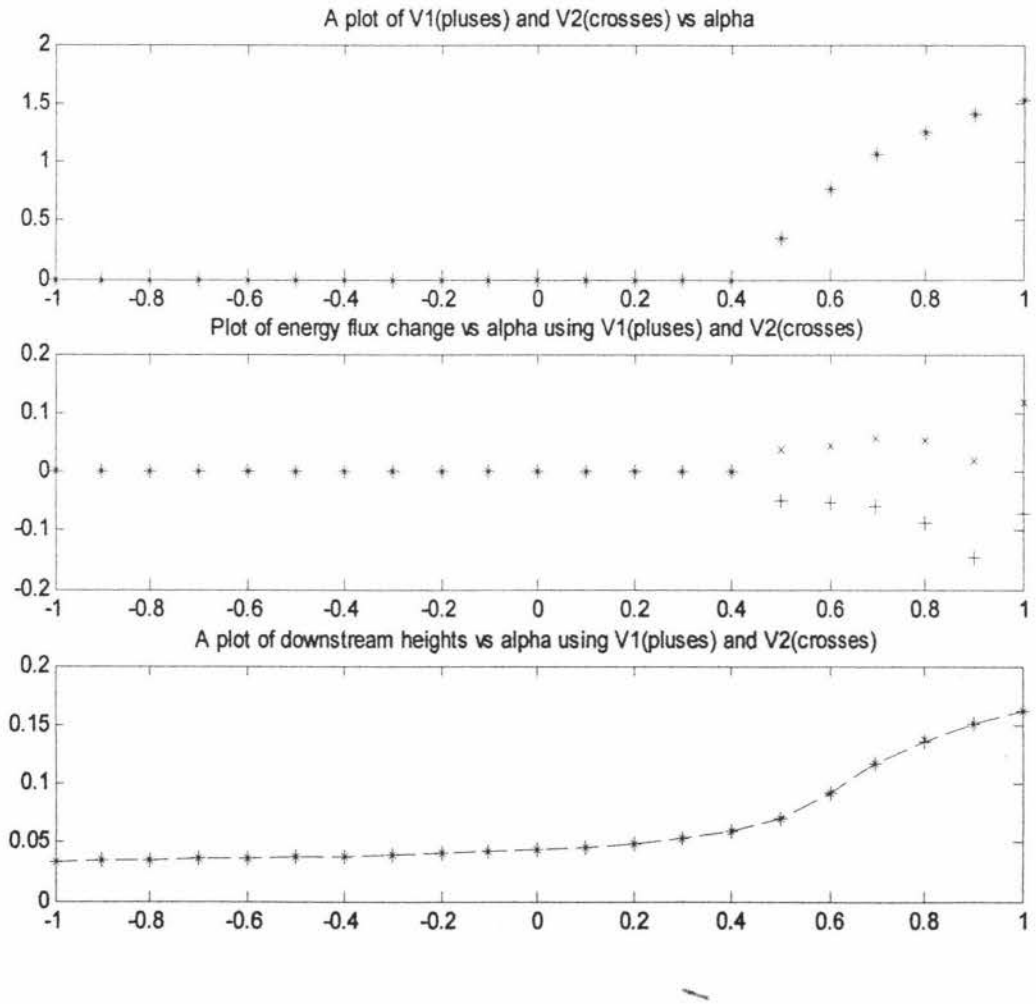

Figure 2 - Plots of downstream height, wave speeds and energy fluxes vs α

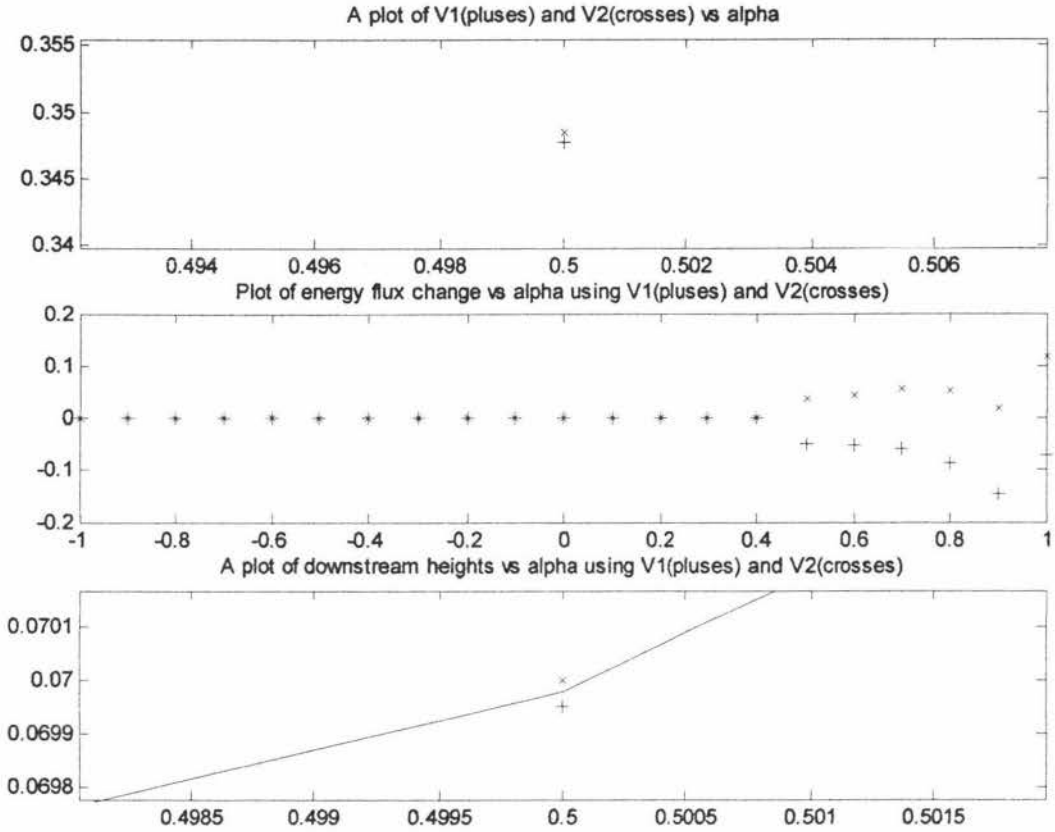

Figure 3 - Zoomed plots of downstream height, wave speeds and energy fluxes vs α

Before we wrap up the single section theory, we should note that there is one more relation we have yet to investigate: energy conservation principle. Like the momentum conservation relation, for a specific region of the fluid system:

changes in mechanical energy fluxes = net work rate of the forces

It should be pointed out that we are focusing on mechanical energy fluxes because of the assumptions employed in this analysis: negligible thermal effects, no significant internal energy changes within each fluid layer. Furthermore, the LHS of the above relation can be simply expressed as $\left[\frac{1}{2}\rho_1 A_1 u_1^3 + \frac{1}{2}\rho_2 A_2 u_2^3\right]_{z_1}^{z_2}$ since we do not know the exact conditions inside the travelling jump, specifically how the forces are behaving in this jump region, However, we are able to quantify the overall energy flux change due to the jump. This is useful because it allows us to determine whether a certain transition is feasible or not. Assuming that there is no energy added to the system, we should have a energy flux loss due to the travelling jump.

3.4 Multiple Section theory: A comparison of conceptual models

Our last segment for this chapter will look at the problem where we have a moving jump across a junction between two sections. We shall outline two models and present its merits and highlight the areas in which the model breaks down (if applicable). Note that we shall present the conceptual models at this stage.

Theory 1: Dissipation of travelling jump across two consecutive pipe sections.

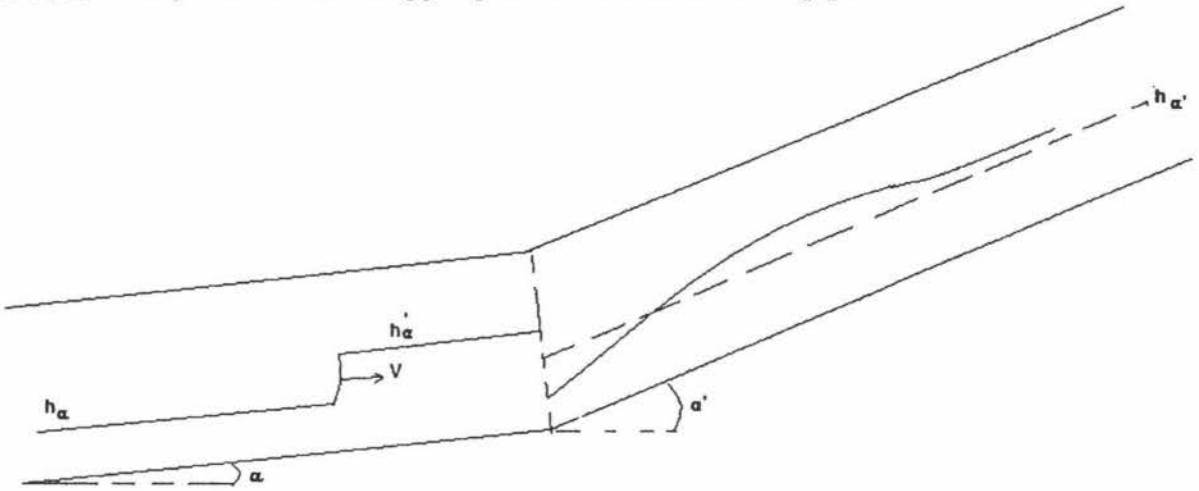

Figure 4 - A sketch of theory 1

Our travelling jump consists of two parts: upstream and downstream components. As it crosses the junction, the downstream section will enter the α' section. According to the long wave theory, which we shall look into in the next chapter, the downstream height h_1' will asymptotically approach the uniform depth for the α' section. The same will apply to the upstream depth as it enters the α' section.

We know that this is in line with previously developed theories because the uniform depth is unique to the angle of inclination. Hence, the implication of this model is that the travelling jump/wave will dissipate and stretch into a long stationary wave.

Theory 2: Preservation of volume fluxes across two consecutive pipe sections.

This model insists that the volume fluxes that leave the α section will also enter the α' section and that the incoming volume fluxes will be preserved throughout the α' section. We assume that there is no sudden transition at the junction.

It appears plausible because of the conservation of mass principle. What comes out of α section must go into α' section. However, this model breaks down because the manner in which the travelling jump is subsequently transported in the α' section is unknown.

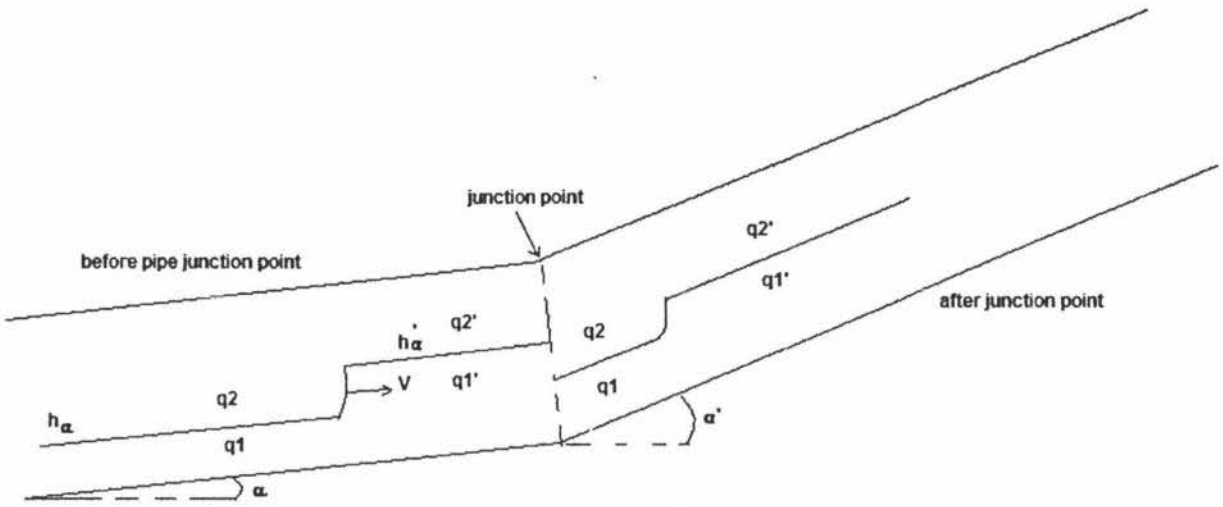

Figure 5 - A sketch of theory 2

Unlike previous occasions, we know the volume fluxes (upstream and downstream) in the α' section whereas before, we had to determine the downstream conditions, given upstream data. This allows us to individually calculate the upstream and downstream heights, thus forming a 'wave'. However, we have yet to establish whether the resulting 'wave' is sustainable as we need to check to see if the downstream volume fluxes tallies with the results obtained from the single section theory for the α' section. If they do, then such a 'wave' is theoretically feasible.

3.5 Closing Remarks

In this chapter, we seek to find the conditions by which a travelling jump can exist in a single pipe section (see figure 1a). To simplify the problem, we imagined that we were moving with the travelling jump and then consider the entire system relative to the travelling jump (see figure 1b).

Our travelling jump is assumed to have a uniform flow condition before (upstream) and ahead (downstream) of the jump. We assumed that the upstream condition was known beforehand and sought to determine the corresponding downstream height, if it exists. As the jump region is assumed to be small, it enabled us to neglect some of the terms in the momentum balance equation such as the gravitational and wall shear components in this jump zone. If the downstream and upstream interfacial depths are equal, then we can conclude that there is no travelling wave that can exist in the pipe section, subject to those specific operational conditions.

This chapter was concluded with the conceptual modelling of the motion of a travelling jump across two sections. The ones described here refer to the As we will show in Chapter 4, the travelling jump dissipation theory is the best model because of the characteristic of the two-layered flow, i.e. a tendency to approach the uniform depth condition.

Chapter 4

LONG WAVE PROBLEM

4.1 INTRODUCTION

In this chapter, we will consider the scenario where we will allow a small axial interfacial gradient. This extends the theories developed in chapter 1. In this chapter, we shall look at the feasibility of long waves existing in the pipe section by allowing a small axial interfacial gradient. This means *h(z)* is not a constant. A sketch of the problem at hand is given in Figure 1a.

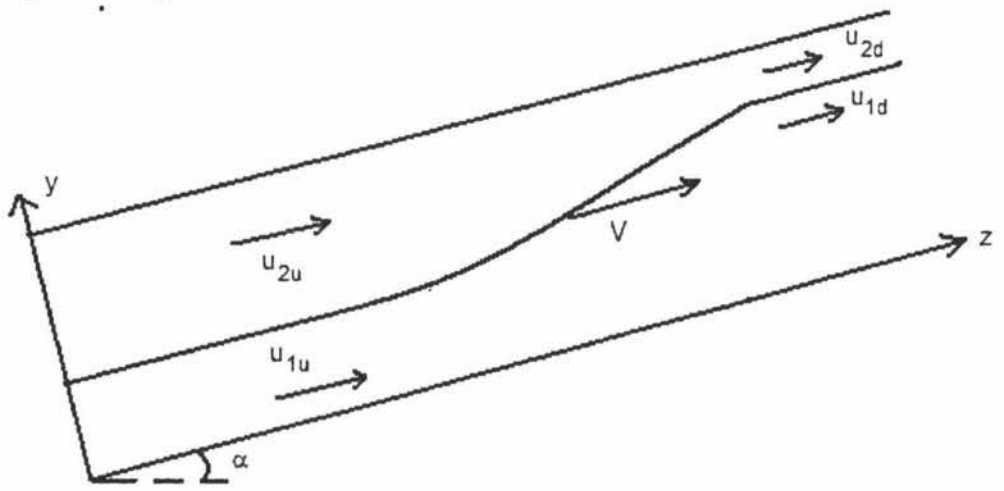

Figure 1a - A sketch of actual long wave scenario

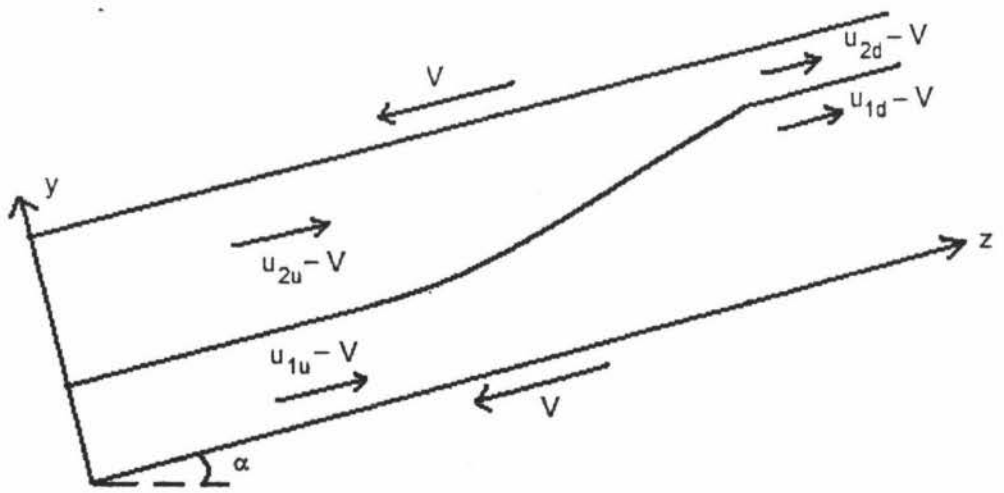

Figure 1b - A sketch of long wave scenario: fluids' relative speeds to a possible travelling wave

We shall now highlight the assumptions employed in this problem.

i. Interface, h varies along z and is a smooth transition from one uniform regime (upstream) to another (downstream).

ii. Interfacial slope changes are negligible => surface tension effects are negligible.

iii. Shallow water approximation will be employed => wavelength of interface >> interfacial layer depth

iv. Uniform flow regime before (upstream) and after (downstream) the long wave.

v. Long wave's speed, V, is constant.

vi. Thermal effects and any internal energy changes in the fluid are negligible.

Our goals of this chapter are as follows.

i. Plot the interface that describes the long wave scenario.

ii. Find a possible expression for V and to determine whether it is feasible to have a travelling wave or a stationary wave.

4.2 Derivation of Equations

As before, we shall solve this problem using first principles: conservation relations of mass, momentum and energy. For the conservation of mass, we will follow the same approach as in Chapter 3.

We now turn to the conservation of momentum relation. Unlike in the travelling jump scenario, we now need to include all the forces that exist in this region bounding the interfacial variation. Taking the calculus approach, we shall turn our attention to a small slice of length Δz of the desired region and quantify every force and their corresponding terms.

This principle states that any changes in the momentum flux profile are due to the forces at work to induce this profile change. There are 4 force terms along with the momentum flux term as detailed in Table 3. Let $z^* \in [z, z + \Delta z]$ be some point in this infinitesimal slice.

Table 3: Components of Momentum Conservation Relation

Term	Fluid Layer 1	Fluid Layer 2
Wall Shear Force	$\tau_1 S_1 \Delta z\big\vert_z$.	$\tau_2 S_2 \Delta z\big\vert_z$.
Interfacial Shear Force	$\tau_{i1} S_i \Delta z\big\vert_z$.	$\tau_{i2} S_i \Delta z\big\vert_z$.
Body Force	$\rho_1 A_1 g \sin(\alpha)\big\vert_z$.	$\rho_2 A_2 g \sin(\alpha)\big\vert_z$.
Pressure Force	$-\frac{dP_{i1}}{dz} A_1 \Delta z - \rho_1 g \cos(\alpha) \frac{dh}{dz} A_1 \Delta z\Big\vert_z$.	$-\frac{dP_{i2}}{dz} A_2 \Delta z - \rho_2 g \cos(\alpha) \frac{dh}{dz} A_2 \Delta z\Big\vert_z$.
Momentum flux	$\rho_1 A_1 (u_1 - V)^2\big\vert_z^{z+\Delta z}$	$\rho_2 A_2 (u_2 - V)^2\big\vert_z^{z+\Delta z}$

We are able to characterise the terms on a layer by layer basis because of the assumption that this long transition (long wave), from one uniform regime to another, is a smooth one, in contrast to the travelling jump scenario where we cannot make such an assumption because the manner by which this travelling jump is induced is not known. Furthermore, we shall characterise the relative average fluid speeds by general functions, $u_1 - V$ and $u_2 - V$.

All the terms are apparent from previously developed definitions of shear and wetted perimeters, except for the pressure force terms. So, we shall take the opportunity to do so now.

From the shallow water approximation, the pressure at each phase is hydrostatic (i.e. depends on gravity). We shall use the interfacial pressure instead of the averaged pressures because it will be easier to illustrate the forces. Surface tension effects are due to the curvature of the interface, so the averaged pressures will be different from the interfacial pressures, P_{i1} and P_{i2}. As the interfacial gradients are assumed to be very small, we will then have $\frac{\partial^2 h}{\partial z^2} << 1 \Rightarrow P_{i1} = P_{i2}$. The interfacial pressure, P_{i1} is acting perpendicular to the interface. However since we are working with terms acting along the axis of the pipe section (z-axis), we shall consider the z-component of this interfacial pressure force. We should include the angle this infinitesimal slice of interface makes with the horizontal z-axis but by our assumption, this angle is close to zero, allowing us to take $P_{i1} \Delta A_1$ as the force acting on the extra bit of cross-sectional area at $z + \Delta z$, as shown in Figure 2.

We want to find the net pressure force but we need to expand the pressure force terms at $z + \Delta z$. Referring to Figure 2, we note that the terms shown in (4.1a) and (4.1b) are evaluated at some point $z^* \in [z, z + \Delta z]$

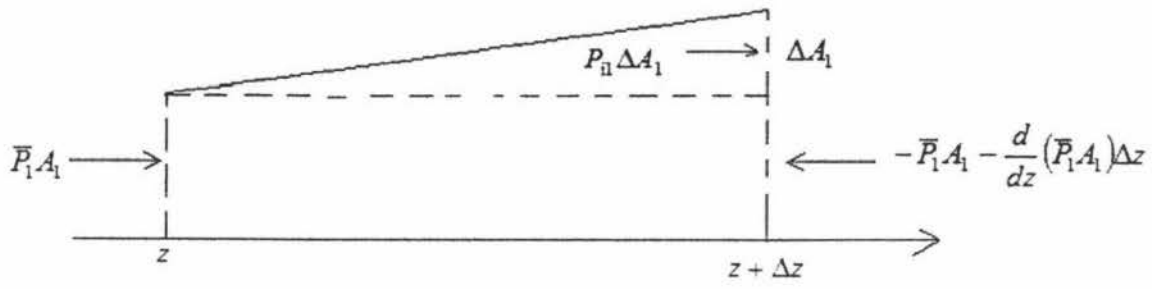

Figure 2 - An exaggerated sketch of the pressure forces at z and $z + \Delta z$ for liquid 1

Expanding the gradient of the pressure force, we obtain:

$$\frac{d}{dz}(\overline{P}_1 A_1) = \frac{d}{dz} \iint_{A_1} (P_{i1} + \rho_1 g(h-y)\cos(\alpha))\ dA$$

$$= \frac{d}{dz}(P_{i1} A_1) + \rho_1 g \cos(\alpha)\frac{dh}{dz} A_1 \qquad (4.1a)$$

$$\frac{d}{dz}(\overline{P}_2 A_2) = \frac{d}{dz} \iint_{A_2} (P_{i2} - \rho_2 g(y-h)\cos(\alpha))\ dA$$

$$= \frac{d}{dz}(P_{i2} A_2) + \rho_2 g \cos(\alpha)\frac{dh}{dz} A_2 \qquad (4.1b)$$

From (4.1a) and (4.1b), we can now begin to sum the net pressure force for each fluid layer across this slice, where k = 1, 2.

$$\Delta F^{net}_{pressure,k} = -\frac{d}{dz}(\overline{P}_k A_k)\Delta z + P_{ik}\Delta A_k$$

$$\Delta F^{net}_{pressure,k} = -\frac{d}{dz}(P_{ik} A_k)\Delta z + P_{ik}\Delta A_k - \rho_k g \cos(\alpha)\frac{dh}{dz} A_k$$

$$\Delta F^{net}_{pressure,k} = -\frac{dP_{ik}}{dz}(A_k)\Delta z - P_{ik}\frac{dA_k}{dz}\Delta z + P_{ik}\Delta A_k - \rho_k g \cos(\alpha)\frac{dh}{dz} A_k \qquad (4.2)$$

When we divide the equation above by Δz , $\Delta z \rightarrow 0$ and setting and applying to both layer 1 and 2, we will then obtain the following relations for the pressure forces, as shown in the table 3 of the momentum flux terms.

$$\frac{dF^{net}_{pressure,k}}{dz} = -\frac{dP_{ik}}{dz}(A_k) - \rho_k g \cos(\alpha)\frac{dh}{dz} A_k \qquad (4.3)$$

So, having explained all the terms, we shall now construct our momentum flux equation for both liquids 1 and 2.

$$\frac{d}{dz}\left(\rho_1 A_1 (u_1 - V)^2\right) = -\rho_1 A_1 g \sin(\alpha) - \tau_1 S_1 + \tau_i S_i - \frac{dP_{i1}}{dz}(A_1) - \rho_1 g \cos(\alpha)\frac{dh}{dz} A_1 \quad (4.4a)$$

$$\frac{d}{dz}\left(\rho_2 A_2 (u_2 - V)^2\right) = -\rho_2 A_2 g \sin(\alpha) - \tau_2 S_2 - \tau_i S_i - \frac{dP_{i2}}{dz}(A_2) - \rho_2 g \cos(\alpha)\frac{dh}{dz} A_2 \quad (4.4b)$$

(4.4a) and (4.4b) can be simplified and solved for the interfacial gradient, $\frac{dh}{dz}$ but we need to expand the momentum flux terms. The working is detailed below.

$$\begin{aligned}
\frac{d}{dz}\left(\rho_k A_k (u_k - V)^2\right) &= \rho_k\left[\frac{dA_k}{dz}(u_k - V)^2 + A_k \frac{d}{dz}(u_k - V)^2\right] \\
&= \rho_k\left[\frac{dA_k}{dz}(u_k - V)^2 + 2A_k (u_k - V)\frac{du_k}{dz}\right] \\
&= \rho_k\left[\frac{dA_k}{dz}(u_k - V)^2 + 2A_k (u_k - V)\frac{d}{dz}\left(\frac{q_k}{A_k}\right)\right] \\
&= \rho_k\left[\frac{dA_k}{dz}(u_k - V)^2 + 2q_k A_k (u_k - V)\frac{dA_k}{dz}\left(\frac{-1}{A_k^2}\right)\right] \\
&= \rho_k\left[\frac{dA_k}{dz}(u_k - V)^2 - 2(u_k - V)\frac{dA_k}{dz}\left(\frac{q_k}{A_k}\right)\right] \\
&= \rho_k \frac{dA_k}{dh}\frac{dh}{dz}(u_k - V)\left[(u_k - V) - 2u_k\right] \\
&= \rho_k \frac{dA_k}{dh}\frac{dh}{dz}(u_k - V)(-u_k - V) \\
&= -\rho_k \frac{dA_k}{dh}\frac{dh}{dz}(u_k - V)(u_k + V) \quad (4.5)
\end{aligned}$$

where we recall that the area functions (A_1 and A_2) are in terms of h.

Now, we substitute (4.5) into (4.4a) and (4.4b) and equate the 2 interfacial pressure gradients because we have neglected surface tension effects. Then, we solve the resulting equation for $\frac{dh}{dz}$ to obtain.

$$\frac{dh}{dz} = \frac{-\tau_1 S_1 A_2 + \tau_i S_i (A_1 + A_2) + \tau_2 S_2 A_1 + (\rho_2 - \rho_1) g \sin(\alpha)}{\left(\frac{\rho_2 (u_2 - V)(u_2 + V)}{A_2}\right)\frac{dA_2}{dh} - \left(\frac{\rho_1 (u_1 - V)(u_1 + V)}{A_1}\right)\frac{dA_1}{dh} + (\rho_1 - \rho_2) g \cos(\alpha) A_1 A_2} \tag{4.6}$$

Finally to the energy conservation relation, we will neglect the internal energy changes within the fluid molecules and thermal effects as we are assuming that the mechanical energy fluxes (i.e. kinetic energy fluxes) are dominant in this system. The principle is expressed as follows:

change in mechanical energy flux = net work rate of forces in the pipe section

We should note that in considering the average fluid speeds in relation to a possibly travelling wave of constant speed, V, the shear forces are determined using the actual average speeds. This is because the presence of the travelling wave does not affect the bulk flow of the fluid layer. However, in considering the work rate of the force, we need to take the force and multiply it by the relative fluid speeds as we will show below.

$$\frac{d}{dz}\left(\frac{\rho_1 A_1 (u_1 - V)^3}{2}\right) = -\rho_1 A_1 g \sin(\alpha)(u_1 - V) - \tau_1 S_1 (u_1 - V) + \tau_i S_i (u_1 - V) - \frac{dP_{i1}}{dz}(A_1)(u_1 - V) - \rho_1 g \cos(\alpha)\frac{dh}{dz} A_1 (u_1 - V) \tag{4.7a}$$

$$\frac{d}{dz}\left(\frac{\rho_2 A_2 (u_2 - V)^3}{2}\right) = -\rho_2 A_2 g \sin(\alpha)(u_2 - V) - \tau_2 S_2 (u_2 - V) - \tau_i S_i (u_2 - V) - \frac{dP_{i2}}{dz}(A_2)\cdot(u_2 - V) - \rho_2 g \cos(\alpha)\frac{dh}{dz} A_2 \cdot (u_2 - V) \tag{4.7b}$$

Now, we want to follow the same procedure as with the momentum conservation relation and look at the energy flux terms in greater detail where k = 1, 2. Following a procedure similar to the momentum flux computations (equations 4.7a and 4.7b), we get:

$$\frac{d}{dz}\left(\rho_k A_k (u_k - V)^3\right) = \rho_k \left[\frac{dA_k}{dz}(u_k - V)^3 + A_k \frac{d}{dz}(u_k - V)^3\right]$$
$$= \rho_k (u_k - V)^2 \frac{dA_k}{dh}\frac{dh}{dz}(-2u_k - V) \tag{4.8}$$

As we did before, we substitute (4.8) into (4.7a) and (4.7b) and equate the 2 interfacial pressure gradients because we have neglected surface tension effects. Then, we solve the resulting equation for $\frac{dh}{dz}$ to obtain.

$$\frac{dh}{dz} = \frac{-\tau_1 S_1 A_2 + \tau_i S_i (A_1 + A_2) + \tau_2 S_2 A_1 + (\rho_2 - \rho_1) g \sin(\alpha)}{\left(\frac{\rho_2 (u_2 - V)(2u_2 + V)}{2A_2}\right)\frac{dA_2}{dh} - \left(\frac{\rho_1 (u_1 - V)(2u_1 + V)}{2A_1}\right)\frac{dA_1}{dh} + (\rho_1 - \rho_2) g \cos(\alpha) A_1 A_2} \quad (4.9)$$

Comparing (4.6) and (4.9), we see that the sole difference lies in the denominator of these expressions. We know that (4.6) must equal to (4.9) because both refer to the same interface.

$$\left(\frac{\rho_2 (u_2 - V)(2u_2 + V)}{2A_2}\right)\frac{dA_2}{dh} - \left(\frac{\rho_1 (u_1 - V)(2u_1 + V)}{2A_1}\right)\frac{dA_1}{dh} + (\rho_1 - \rho_2) g \cos(\alpha) A_1 A_2$$
$$= \left(\frac{\rho_2 (u_2 - V)(u_2 + V)}{A_2}\right)\frac{dA_2}{dh} - \left(\frac{\rho_1 (u_1 - V)(u_1 + V)}{A_1}\right)\frac{dA_1}{dh} + (\rho_1 - \rho_2) g \cos(\alpha) A_1 A_2 \quad (4.10)$$

4.3 Solution Procedure and Analysis

We also note that given that $A_1 + A_2 = A_c$ (a constant), $\frac{dA_2}{dh} = -\frac{dA_1}{dh}$. So, (4.10) can be simplified to yield:

$$-\left(\frac{\rho_2 (u_2 - V)(2u_2 + V)}{2A_2}\right)\frac{dA_1}{dh} - \left(\frac{\rho_1 (u_1 - V)(2u_1 + V)}{2A_1}\right)\frac{dA_1}{dh}$$
$$= -\left(\frac{\rho_2 (u_2 - V)(u_2 + V)}{A_2}\right)\frac{dA_1}{dh} - \left(\frac{\rho_1 (u_1 - V)(u_1 + V)}{A_1}\right)\frac{dA_1}{dh}$$
$$-\left(\frac{\rho_2 (u_2 - V)(2u_2 + V)}{2A_2}\right) - \left(\frac{\rho_1 (u_1 - V)(2u_1 + V)}{2A_1}\right)$$
$$= -\left(\frac{\rho_2 (u_2 - V)(u_2 + V)}{A_2}\right) - \left(\frac{\rho_1 (u_1 - V)(u_1 + V)}{A_1}\right)$$

$$-\left(\frac{\rho_2 (2u_2^2 - u_2 V - V^2)}{2A_2}\right) - \left(\frac{\rho_1 (2u_1^2 - u_1 V - V^2)}{2A_1}\right) = -\left(\frac{\rho_2 (u_2^2 - V^2)}{A_2}\right) - \left(\frac{\rho_1 (u_1^2 - V^2)}{A_1}\right)$$

$$-\left(\frac{\rho_2 (-u_2 V - V^2)}{2A_2}\right) - \left(\frac{\rho_1 (-u_1 V - V^2)}{2A_1}\right) = -\left(\frac{\rho_2 (-V^2)}{A_2}\right) - \left(\frac{\rho_1 (-V^2)}{A_1}\right)$$

$$-\left(\frac{\rho_2\left(-u_2V-V^2\right)}{2A_2}\right)-\left(\frac{\rho_1\left(-u_1V-V^2\right)}{2A_1}\right) = 0$$

$$\rho_2A_1\left(u_2V+V^2\right) = \rho_1A_2\left(-u_1V-V^2\right) \tag{4.11}$$

From (4.11), we can solve the quadratic equation which will yield 2 solutions for V.

$$V_1 = 0 \;\&\; V_2 = -\left(\frac{\rho_2A_1u_2+\rho_1A_2u_1}{\rho_2A_1+\rho_1A_2}\right)$$

However, we know that V_2 is not possible since in general, V_2 is not a constant which leaves $V = 0$ being the only viable solution. The key conclusion is that we will not be able to have a steady long wave of permanent form unless the transition is short and abrupt as we have found for the travelling jump scenario (Chapter 3).

Having obtained $V = 0$, we can now determine the $\frac{dh}{dz}$ relation which we will use to solve for the plot of the interface and the relation is given below.

$$\frac{dh}{dz} = \frac{-\tau_1S_1A_2 + \tau_iS_i\left(A_1+A_2\right) + \tau_2S_2A_1 - \left(\rho_1-\rho_2\right)gA_1A_2\sin\alpha}{\frac{\rho_2A_1q_2^2}{A_2^2}\frac{dA_2}{dh} - \frac{\rho_1A_2q_1^2}{A_1^2}\frac{dA_1}{dh} + \left(\rho_1-\rho_2\right)g\cos\alpha A_1A_2} \tag{4.12}$$

The details of this MATLAB program is given in D:/Thesis Work/Chapter 4/Linked Pipeline/test_plot.m. Looking at (4.12), we can make the following conclusions.

i. If the downstream and upstream layer depths are the same, then we will have a planar axial interface.

ii. We will have only one uniform layer depth, in contrast to the travelling wave scenario where it was possible to have two depths (upstream and downstream).

iii. If the input height into a pipe section is not the uniform layer depth for that particular pipe section, then the interface will asymptotically approach the uniform flow depth.

4.4 Case Study - Multiple Section Problem

An obvious extension of this theory is to consider the case when we allow a smooth transition between two adjacent pipe sections. This is different from the planar interface scenario (Chapter 2) where we assumed a sudden transition at the junction region to induce uniform flow pattern in the subsequent section. We set the transition

point to be $z = 100$ and note that the bold and dashed lines refer to the α and α' sections respectively and the crosses and starred lines refer to u_1 and u_2 respectively.

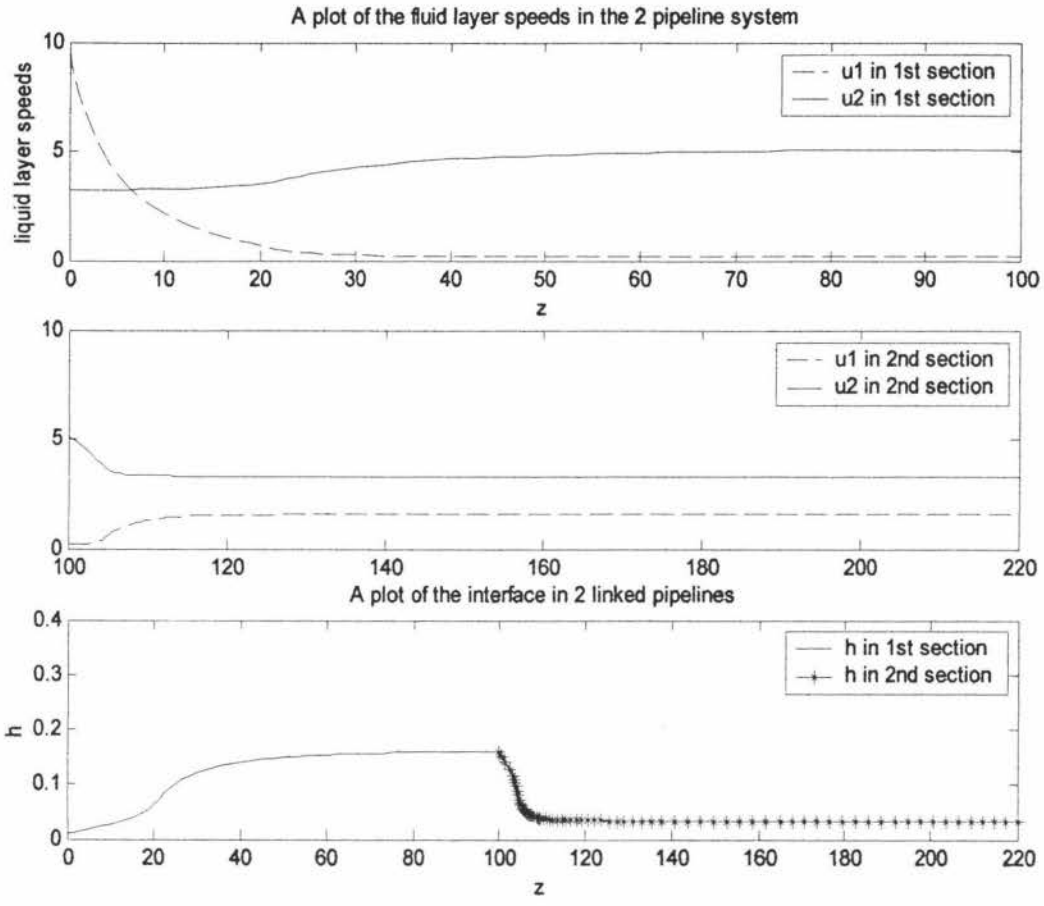

Figure 3 - A case study involving 2 linked pipe sections when $\alpha = 1$, $\alpha' = -1$

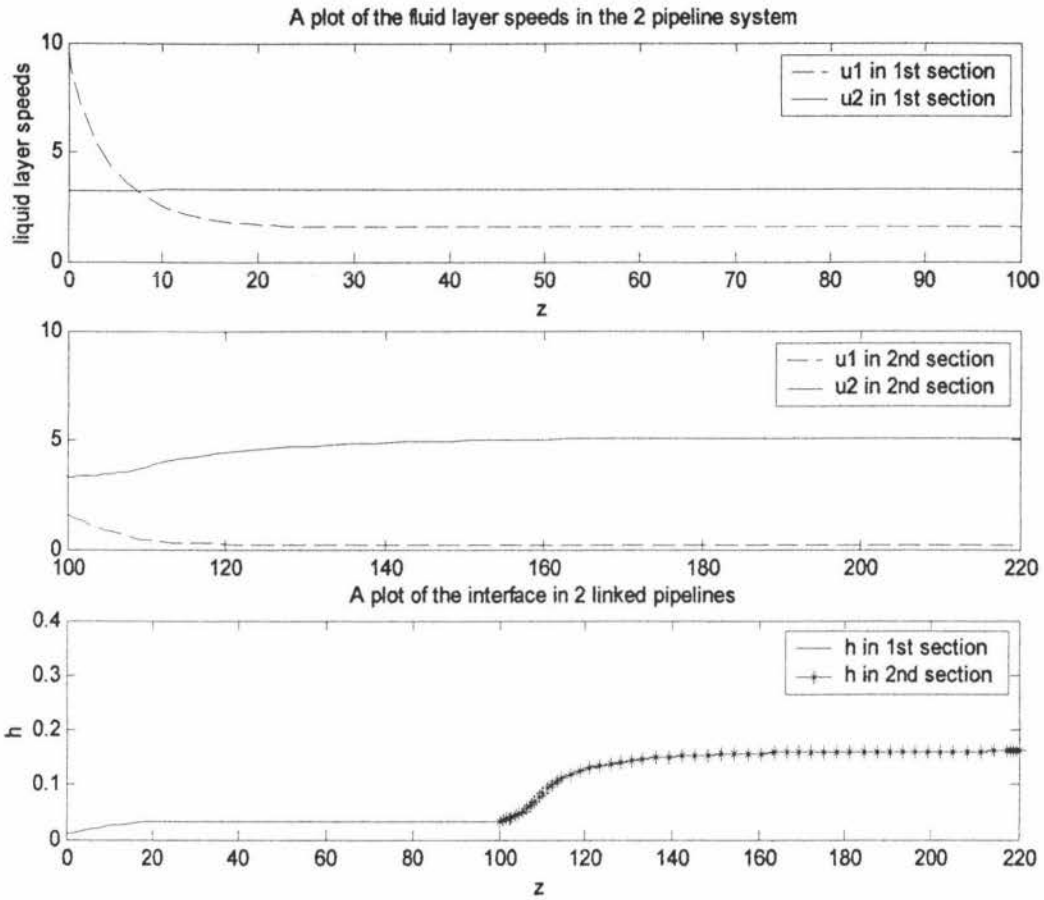

Figure 4 - A case study involving 2 linked pipe sections when $\alpha = -1$, $\alpha' = 1$

We observe that the interfacial depth will asymptotically approach the uniform layer depth for that pipe section. This supports theory 1 of section 3.4, where we theorized that the travelling jump dissipates to the uniform layer depth of the new pipe section as the travelling jump (a short pulse) moves across two pipe sections.

4.5 Closing Remarks

In this chapter, we have extended the axial planar interface model (see Chapter 2) by allowing a small axial interfacial variation. The solution approach that we have adopted is similar to the previous chapter (travelling jump) as we defined this long wave to be composed of three regions: before the wave, long wave itself and after the wave. The flow regime before and after this long wave is assumed to satisfy the uniform flow criterion, namely that the average pressure gradient across both fluid layers are equal.

It has been demonstrated that we do not have a steady long wave of permanent form. Physically, this means that no long wave can propagate in the pipeline. What

happens is that the interface tends to approach the uniform layer depth, i.e. the depth obtained by imposing the uniform flow criterion.

Chapter 5

STABILITY ANALYSIS

5.1 INTRODUCTION

In this chapter, we shall investigate what happens when we introduce a small disturbance to the steady state fluid system, governed by the solution H, U_1 and U_2. As inferred in the chapter title, we want to see if this disturbance is grows (unstable) or decays or remains neutral (stable). We shall investigate the full time dependent momentum equation and employ the time dependent continuity equation, following the method of analysis adopted by [14] and the solution analysis is detailed in the subsequent sections. The main difference between our analysis and that featured in [14, 16] is that we shall neglect surface tension effects.

5.2 DERIVATION OF EQUATIONS

Continuity equations:

$$\frac{\partial}{\partial t}(\rho_1 A_1) + \frac{\partial}{\partial z}(\rho_1 A_1 u_1) = 0 \tag{5.1}$$

$$\frac{\partial}{\partial t}(\rho_2 A_2) + \frac{\partial}{\partial z}(\rho_2 A_2 u_2) = 0 \tag{5.2}$$

Momentum equations:

$$\frac{\partial}{\partial t}(\rho_1 A_1 u_1) + \frac{\partial}{\partial z}(\rho_1 A_1 u_1^2) = -\tau_1 S_1 + \tau_i S_i - \frac{\partial}{\partial z}(\overline{P}_1 A_1) + P_{i1}\frac{\partial A_1}{\partial z} - \rho_1 A_1 g \sin(\alpha) \tag{5.3}$$

$$\frac{\partial}{\partial t}(\rho_2 A_2 u_2) + \frac{\partial}{\partial z}(\rho_2 A_2 u_2^2) = -\tau_2 S_2 + -\tau_i S_i - \frac{\partial}{\partial z}(\overline{P}_2 A_2) + P_{i2}\frac{\partial A_2}{\partial z} - \rho_2 A_2 g \sin(\alpha) \tag{5.4}$$

Using (4.1a) and (4.1b), (5.3) and (5.4) are transformed into.

$$\frac{\partial}{\partial t}(\rho_1 A_1 u_1) + \frac{\partial}{\partial z}(\rho_1 A_1 u_1^2) = -\tau_1 S_1 + \tau_i S_i - A_1 \frac{\partial P_{i1}}{\partial z} - \rho_1 A_1 g \sin(\alpha) - \rho_1 A_1 g \cos(\alpha)\frac{\partial h}{\partial z} \quad (5.5)$$

$$\frac{\partial}{\partial t}(\rho_2 A_2 u_2) + \frac{\partial}{\partial z}(\rho_2 A_2 u_2^2) = -\tau_2 S_2 - \tau_i S_i - A_2 \frac{\partial P_{i2}}{\partial z} - \rho_2 A_2 g \sin(\alpha) - \rho_2 A_2 g \cos(\alpha)\frac{\partial h}{\partial z} \quad (5.6)$$

We shall now do the following

i. Differentiate the terms in the LHS of (5.5) and (5.6).

ii. Substitute the continuity equations and hydrostatic relation for each fluid layer (see 4.1a and 4.1b) into the expanded form of the LHS of (5.5) and (5.6).

iii. Solve (5.5) and (5.6) for the interfacial pressure gradients.

$$\frac{\partial P_{i1}}{\partial z} + \rho_1 \frac{\partial u_1}{\partial t} + \rho_1 u_1 \frac{\partial u_1}{\partial z} = -\frac{\tau_1 S_1}{A_1} + \frac{\tau_i S_i}{A_1} - \rho_1 g \sin(\alpha) - \rho_1 g \cos(\alpha)\frac{\partial h}{\partial z} \quad (5.7)$$

$$\frac{\partial P_{i2}}{\partial z} + \rho_2 \frac{\partial u_2}{\partial t} + \rho_2 u_2 \frac{\partial u_2}{\partial z} = -\frac{\tau_2 S_2}{A_2} - \frac{\tau_i S_i}{A_2} - \rho_2 g \sin(\alpha) - \rho_2 g \cos(\alpha)\frac{\partial h}{\partial z} \quad (5.8)$$

Then, we subtract (5.8) from (5.7) and this yields the combined momentum equation.

$$\left(\rho_1 \frac{\partial u_1}{\partial t} - \rho_2 \frac{\partial u_2}{\partial t}\right) + \left(\rho_1 u_1 \frac{\partial u_1}{\partial z} - \rho_2 u_2 \frac{\partial u_2}{\partial z}\right) + (\rho_1 - \rho_2) g \cos(\alpha)\frac{\partial h}{\partial z} = \sigma \quad (5.9)$$

where we shall define

$$\sigma = -\frac{\tau_1 S_1}{A_1} + \frac{\tau_2 S_2}{A_2} + \tau_i S_i\left(\frac{1}{A_1} + \frac{1}{A_2}\right) - (\rho_1 - \rho_2) g \sin(\alpha)$$

5.3 ANALYSIS OF PERTURBATION VARIABLES

Now, we assume that H, U_1 and U_2 define the solution to the time independent problem and so we also assume that h^*, u_1^*, u_2^* are the perturbed variables where $\frac{h^*}{H}$, $\frac{u_1^*}{U_1}$, $\frac{u_2^*}{U_2} << 1$.

It should be noted that the perturbed variables will give us a clue to the instability and neutral stability criterion for the specified flow parameters.

First, we make the substitutions for h, u_1 and u_2 as follows: $h = H + h^*$, $u_1 = U_1 + u_1^*$, $u_2 = U_2 + u_2^*$.

Second, we shall substitute the perturbed parameters and linearize (*5.1*), (*5.2*) and (*5.9*) accordingly. We recall that H, U_1 and U_2 solves the time independent version of (*5.9*) and so satisfies the continuity relation. We shall work out the case for (*5.1*) as (*5.2*) is similar.

$$(5.1) \Rightarrow \rho_1 \frac{\partial A_1}{\partial h}\frac{\partial h}{\partial t} + \rho_1 \frac{\partial}{\partial z}(A_1 u_1) = 0$$

$$\Rightarrow \rho_1 A_1' \frac{\partial h}{\partial t} + \rho_1 A_1 \frac{\partial u_1}{\partial z} + \rho_1 u_1 \frac{\partial A_1}{\partial z} = 0$$

$$\Rightarrow A_1' \frac{\partial}{\partial t}(h^* + H) + A_1 \frac{\partial}{\partial z}(u_1^* + U_1) + (u_1^* + U_1)\frac{\partial A_1}{\partial h}\frac{\partial}{\partial z}(h^* + H) = 0$$

$$\Rightarrow A_1' \frac{\partial h^*}{\partial t} + A_1 \frac{\partial u_1^*}{\partial z} + U_1 \frac{\partial A_1}{\partial h}\frac{\partial h^*}{\partial z} = 0 \qquad (5.10)$$

Similarly, we have for the 2nd fluid layer, with $A_2' = -A_1'$ $\because A_1 + A_2 =$ constant

$$-A_1' \frac{\partial h^*}{\partial t} + A_2 \frac{\partial u_2^*}{\partial z} - U_2 \frac{\partial A_1}{\partial h}\frac{\partial h^*}{\partial z} = 0 \qquad (5.11)$$

Turning finally to the momentum equation, we shall employ the same method as used to obtain (5.10) and (5.11). First, we find a Taylor expansion of σ about the point (H, U_1, U_2), we will then obtain.

$$\sigma(h,u_1,u_2) = \sigma(H,U_1,U_2) + (h-H)\frac{\partial\sigma}{\partial h}\Big|_{h=H} + (u_1-U_1)\frac{\partial\sigma}{\partial u_1}\Big|_{h=H} + (u_2-U_2)\frac{\partial\sigma}{\partial u_2}\Big|_{h=H}$$

Then, we turn to equation (5.9) with the substituted perturbed variables.

$$\left(\rho_1\frac{\partial}{\partial t}(u_1^{\bullet}+U_1) - \rho_2\frac{\partial}{\partial t}(u_2^{\bullet}+U_2)\right) + (\rho_1-\rho_2)g\cos(\alpha)\frac{\partial}{\partial z}(h^{\bullet}+H)$$
$$+ \left(\rho_1(u_1^{\bullet}+U_1)\frac{\partial}{\partial z}(u_1^{\bullet}+U_1) - \rho_2(u_2^{\bullet}+U_2)\frac{\partial}{\partial z}(u_2^{\bullet}+U_2)\right) = \sigma$$

We see that the H, U_1 and U_2 terms will solve $\sigma(H, U_1, U_2)$ and after we have linearized the equation, i.e. throwing away the perturbed term expressions which are of second order and above, we obtain.

$$\Rightarrow \left(\rho_1\frac{\partial u_1^{\bullet}}{\partial t} - \rho_2\frac{\partial u_2^{\bullet}}{\partial t}\right) + \left(\rho_1U_1\frac{\partial u_1^{\bullet}}{\partial z} - \rho_2U_2\frac{\partial u_2^{\bullet}}{\partial z}\right) + (\rho_1-\rho_2)g\cos(\alpha)\frac{\partial h^{\bullet}}{\partial z}$$
$$(h-H)\frac{\partial\sigma}{\partial h}\Big|_{h=H} + (u_1-U_1)\frac{\partial\sigma}{\partial u_1}\Big|_{u_1=U_1} + (u_2-U_2)\frac{\partial\sigma}{\partial u_2}\Big|_{u_2=U_2}$$
$$\Rightarrow \left(\rho_1\frac{\partial u_1^{\bullet}}{\partial t} - \rho_2\frac{\partial u_2^{\bullet}}{\partial t}\right) + \left(\rho_1U_1\frac{\partial u_1^{\bullet}}{\partial z} - \rho_2U_2\frac{\partial u_2^{\bullet}}{\partial z}\right) + (\rho_1-\rho_2)g\cos(\alpha)\frac{\partial h^{\bullet}}{\partial z}$$
$$= h^{\bullet}\frac{\partial\sigma}{\partial h}\Big|_{h=H} + u_1^{\bullet}\frac{\partial\sigma}{\partial u_1}\Big|_{u_1=U_1} + u_2^{\bullet}\frac{\partial\sigma}{\partial u_2}\Big|_{u_2=U_2} \qquad (5.12)$$

Now, (5.10), (5.11) and (5.12) can be expressed in a single matrix equation given below.

$$\left(T\frac{\partial}{\partial t} + X\frac{\partial}{\partial z}\right)\hat{\eta} = G\hat{\eta} \qquad (5.13)$$

where the terms are defined as follows:

$$T = \begin{pmatrix} A_1' & 0 & 0 \\ -A_1' & 0 & 0 \\ 0 & \rho_1 & \rho_2 \end{pmatrix}, \quad G = \begin{pmatrix} 0 & 0 & 0 \\ 0 & 0 & 0 \\ \frac{\partial\sigma}{\partial H} & \frac{\partial\sigma}{\partial U_2} & \frac{\partial\sigma}{\partial U_2} \end{pmatrix},$$

$$X = \begin{pmatrix} A_1'U_1 & A_1 & 0 \\ -A_1'U_2 & 0 & A_2 \\ (\rho_1-\rho_2)g\cos(\alpha) & \rho_1U_1 & \rho_2U_2 \end{pmatrix} \text{ and } \hat{\eta} = \begin{pmatrix} h^* \\ u_1^* \\ u_2^* \end{pmatrix}$$

We can convert (5.13) into $M\hat{\eta} = 0$, where $M = \left(T\frac{\partial}{\partial t} + X\frac{\partial}{\partial z} - G\right)$

Recalling elementary linear algebra, we know that $M\hat{\eta} = 0$ has a non-trivial solution when *det* $(M) = 0$. Now, we shall make further assume that the perturbation terms have the form of a travelling wave where γ is the real wave number, γc is the complex angular velocity, c is the speed of the propagating disturbance and $\hat{h}, \hat{u}_1, \hat{u}_2$ are the amplitudes of the perturbations.

$$h^* = \hat{h}e^{(i\gamma(z-ct))}$$

$$u_1^* = \hat{u}_1e^{(i\gamma(z-ct))}$$

$$u_2^* = \hat{u}_2e^{(i\gamma(z-ct))}$$

As the form of c is unknown, we shall assume that c has the general form: $c = c_r + ic_i$ with c_r and c_i being the real and complex components of the propagation speed respectively. However, we shall leave the propagation speed term as c for the time being until we consider the analysis of the stability equation, discussed in Section 5.4 where the significance of c_r and c_i will then be looked into.

After we substitute the above relations into (5.10), (5.11) and (5.12), we obtain:

$$(5.10) \Rightarrow A_1'\hat{h}(-i\gamma c) + A_1'U_1\hat{h}(i\gamma) + A_1\hat{u}_1(i\gamma) = 0$$

$$\Rightarrow A_1'(U_1-c)\hat{h} + A_1\hat{u}_1 = 0 \qquad (5.14)$$

$$(5.11) \Rightarrow -A_1'\hat{h}(-i\gamma c) - A_1'U_1\hat{h}(i\gamma) + A_2\hat{u}_2(i\gamma) = 0$$

$$\Rightarrow -A_1'(U_1-c)\hat{h} + A_2\hat{u}_2 = 0 \qquad (5.15)$$

$$(5.12) \Rightarrow (\rho_1\hat{u}_1 - \rho_2\hat{u}_2)(-i\gamma c) + (\rho_1U_1\hat{u}_1 - \rho_2U_2\hat{u}_2)(i\gamma) + (\rho_1-\rho_2)(i\gamma)g\cos(\alpha)\hat{h}$$
$$= \hat{h}\frac{\partial\sigma}{\partial h}\bigg|_{h=H} + \hat{u}_1\frac{\partial\sigma}{\partial u_1}\bigg|_{u_1=U_1} + \hat{u}_2\frac{\partial\sigma}{\partial u_2}\bigg|_{u_2=U_2}$$

$$\Rightarrow \quad (\rho_1\hat{u}_1 - \rho_2\hat{u}_2)(-c) \;+\; (\rho_1 U_1\hat{u}_1 - \rho_2 U_2\hat{u}_2) \;+\; (\rho_1 - \rho_2)g\cos(\alpha)\hat{h}$$
$$= \quad \frac{\hat{h}}{i\gamma}\frac{\partial\sigma}{\partial h}\bigg|_{h=H} \;+\; \frac{\hat{u}_1}{i\gamma}\frac{\partial\sigma}{\partial u_1}\bigg|_{u_1=U_1} \;+\; \frac{\hat{u}_2}{i\gamma}\frac{\partial\sigma}{\partial u_2}\bigg|_{u_2=U_2}$$

$$\Rightarrow \quad \hat{h}\left[(\rho_1 - \rho_2)g\cos(\alpha) + \frac{i}{\gamma}\frac{\partial\sigma}{\partial h}\bigg|_{h=H}\right] \;+\; \hat{u}_1\left[-\rho_1 c + \rho_1 U_1 + \frac{i}{\gamma}\frac{\partial\sigma}{\partial u_1}\bigg|_{u_1=U_1}\right]$$
$$+ \quad \hat{u}_2\left[\rho_2 c - \rho_2 U_2 + \frac{i}{\gamma}\frac{\partial\sigma}{\partial u_2}\bigg|_{u_2=U_2}\right] \;=\; 0 \qquad (5.16)$$

So, our matrix M looks like:

$$M \;=\; \begin{pmatrix} A_1'(U_1 - c) & A_1 & 0 \\ -A_1'(-U_2 + c) & 0 & A_2 \\ (\rho_1 - \rho_2)g\cos(\alpha) + \frac{i}{\gamma}\frac{\partial\sigma}{\partial h}\Big|_{h=H} & -\rho_1 c + \rho_1 U_1 + \frac{i}{\gamma}\frac{\partial\sigma}{\partial u_1}\Big|_{u_1=U_1} & \rho_2 c - \rho_2 U_2 + \frac{i}{\gamma}\frac{\partial\sigma}{\partial u_2}\Big|_{u_2=U_2} \end{pmatrix}$$

To ensure that we do not get a trivial solution for $\begin{pmatrix} \hat{h} \\ \hat{u}_1 \\ \hat{u}_2 \end{pmatrix}$, we must have

det $(M) = 0$.

$$\Rightarrow \quad -A_1'(c - U_1)\left[-A_2\left(-\rho_1 c + \rho_1 U_1 + \frac{i}{\gamma}\frac{\partial\sigma}{\partial U_1}\right)\right] \;-\; A_1\left[-A_2(\rho_1 - \rho_2)g\cos(\alpha) + \frac{i}{\gamma}\frac{\partial\sigma}{\partial H}\right]$$
$$-\; A_1(-A_1'(-U_2 + c))\left(\rho_2 c - \rho_2 U_2 + \frac{i}{\gamma}\frac{\partial\sigma}{\partial U_2}\right) \;=\; 0$$

Simplifying the above equation and grouping terms according to c, we obtain:

$$c^2\left(\rho_1\frac{A_1'}{A_1} + \rho_2\frac{A_1'}{A_2}\right) \;+\; c\left[-2\left(\rho_1 U_1\frac{A_1'}{A_1} + \rho_2 U_2\frac{A_1'}{A_2}\right) + i\left(-\frac{A_1'}{A_1\gamma}\frac{\partial\sigma}{\partial U_1} + \frac{A_1'}{A_2\gamma}\frac{\partial\sigma}{\partial U_2}\right)\right]$$
$$\left[\left(\rho_1 U_1^2\frac{A_1'}{A_1} + \rho_2 U_2^2\frac{A_1'}{A_2} - (\rho_1 - \rho_2)g\cos(\alpha)\right) + i\left(\frac{U_1 A_1'}{A_1\gamma}\frac{\partial\sigma}{\partial U_1} - \frac{U_2 A_1'}{A_2\gamma}\frac{\partial\sigma}{\partial U_2} - \frac{1}{\gamma}\frac{\partial\sigma}{\partial H}\right)\right] \;=\; 0$$

To make things easier for us, we shall define the constituents of the above quadratic equation in c:

$$a = \rho_1 \frac{A_1'}{A_1} + \rho_2 \frac{A_1'}{A_2}$$

$$b_1 = -2\left(\rho_1 U_1 \frac{A_1'}{A_1} + \rho_2 U_2 \frac{A_1'}{A_2} \right)$$

$$b_2 = -\frac{A_1'}{A_1 \gamma} \frac{\partial \sigma}{\partial U_1} + \frac{A_1'}{A_2 \gamma} \frac{\partial \sigma}{\partial U_2}$$

$$d_1 = \rho_1 U_1^2 \frac{A_1'}{A_1} + \rho_2 U_2^2 \frac{A_1'}{A_2} - (\rho_1 - \rho_2) g \cos(\alpha)$$

$$d_2 = \frac{U_1 A_1'}{A_1 \gamma} \frac{\partial \sigma}{\partial U_1} - \frac{U_2 A_1'}{A_2 \gamma} \frac{\partial \sigma}{\partial U_2} - \frac{1}{\gamma} \frac{\partial \sigma}{\partial H}$$

$$\Rightarrow \quad a(c_r + c_i)^2 + (c_r + c_i)(b_1 + ib_2) + (d_1 + id_2) = 0 \qquad (5.17)$$

A plot of these terms for α ranging from -2 to 2 degrees is given.

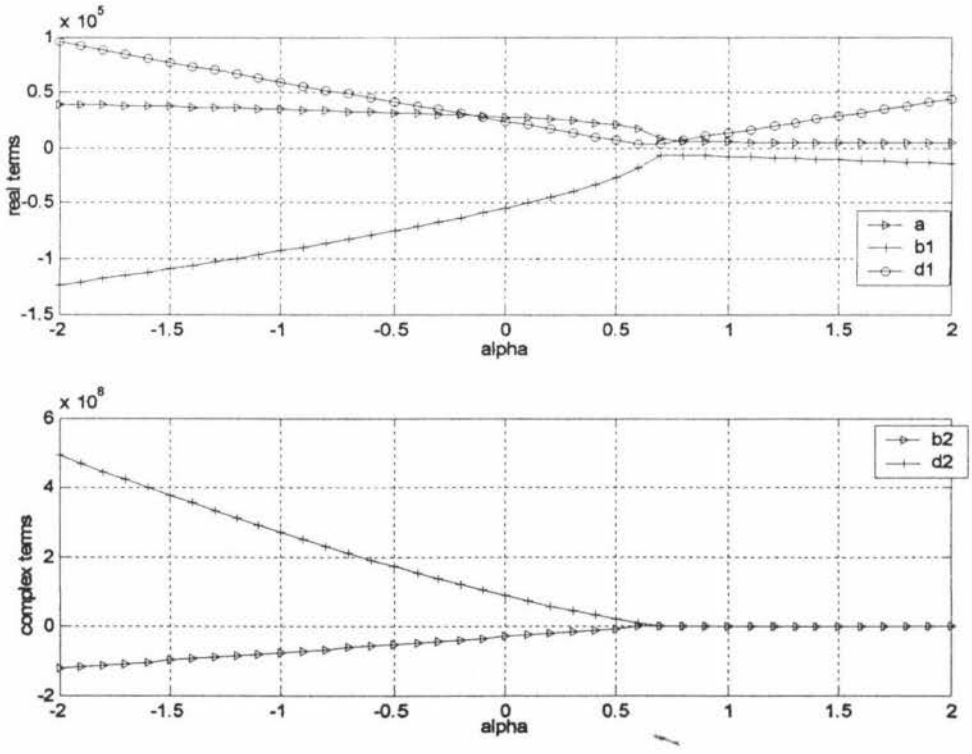

Figure 1 - A plot of the terms in (5.17)

Expanding (5.17) and separating the real and complex terms e_1 and e_2 respectively, we obtain the following:

$$ac_r^2 + b_1c_r + \left(-ac_i^2 - b_2c_i + d_1\right) + i\left(2ac_rc_i + b_2c_r + b_1c_i + d_2\right) = 0 \qquad (5.18)$$

where we have $e_1 = ac_r^2 + b_1c_r + \left(-ac_i^2 - b_2c_i + d_1\right)$ and $e_2 = 2ac_rc_i + b_2c_r + b_1c_i + d_2$.

If we look at the nature of the terms, b_2 and d_2, we see that for disturbances with large wave numbers, γ, i.e. very short waves, the shear force and gravitational terms lose their significance in the analysis. For the next section, we shall denote (5.18) as the stability equation.

5.4 ANALYSIS OF STABILITY EQUATION

Recalling the exponential terms in h^*, u_1^* and u_2^*, we now expand the propagation speed term into its real and complex constituents within the exponential portion of the perturbation terms as shown below:

$$e^{(i\gamma(z-ct))} = e^{(i\gamma(z-(c_r+ic_i)t))} = e^{(i\gamma(z-c_rt))}e^{\gamma c_it}.$$

The term, $e^{i\gamma(z-c_rt)}$ defines the oscillatory nature of the perturbation term, while $e^{\gamma c_it}$ regulates the growth or decay of the perturbation variable. In this section, we want to investigate the significance of the terms: c_r and c_i.

First, we equate the real and complex constituents of (5.18), e_1 and e_2 respectively to 0, we shall now consider two approaches: (1) obtain c_i in terms of c_r and then solve for c_r (see Section 5.4a) and (2) obtain c_r in terms of c_i and then solve for c_i (see Section 5.4b). The condition for neutral stability, i.e. when $c_i = 0$, shall be considered in Section 5.4c.

5.4a Solution of c_r and implication on c_i

$$e_2 = 0 \Rightarrow 2ac_rc_i + b_2c_r + b_1c_i + d_2 = 0 \Rightarrow c_i = \frac{-b_2\left(c_r + \dfrac{d_2}{b_2}\right)}{2a\left(c_r + \dfrac{b_1}{2a}\right)}$$

Now, we substitute c_i, as shown above, into e_1 in (5.18) and we get:

$$ac_r^2 + b_1 c_r - a\left(\frac{-b_2\left(c_r + \frac{d_2}{b_2}\right)}{2a\left(c_r + \frac{b_1}{2a}\right)}\right)^2 - b_2\left(\frac{-b_2\left(c_r + \frac{d_2}{b_2}\right)}{2a\left(c_r + \frac{b_1}{2a}\right)}\right) + d_1 = 0 \qquad (5.19)$$

We shall now multiply (5.19) by the term $2a\left(c_r + \frac{b_1}{2a}\right)$ because we do not want the equation to have any singularity. So, (5.19) becomes

$$\left(ac_r^2 + b_1 c_r + d_1\right)\left(2a\left(c_r + \frac{b_1}{2a}\right)\right)^2 - a\left(-b_2\left(c_r + \frac{d_2}{b_2}\right)\right)^2 - b_2\left(-b_2\left(c_r + \frac{d_2}{b_2}\right)\right)\left(2a\left(c_r + \frac{b_1}{2a}\right)\right) = 0$$

$$\left(ac_r^2 + b_1 c_r + d_1\right)(2ac_r + b_1)^2 - a(b_2 c_r + d_2)^2 + b_2(b_2 c_r + d_2)(2ac_r + b_1) = 0 \qquad (5.20)$$

From (5.20), we can want to investigate what happens to the stability equation at $c_r = -\frac{b_1}{2a}$. We see that when $c_r = -\frac{b_1}{2a}$, (5.20) becomes

$$-a\left(b_2\left(\frac{-b_1}{2a}\right) + d_2\right)^2 = 0 \Rightarrow \frac{d_2}{b_2} = \frac{b_1}{2a} \qquad (5.21)$$

To find the form of the corresponding c_i, we substitute $c_r = -\frac{b_1}{2a}$ into (5.18) and we see that the complex component of (5.18) gives us the same result as (5.21). Turning to the real component of (5.18), we have a quadratic equation in c_i and it is given by

$$ac_i^2 + b_1 c_i - \left(d_1 - \frac{b_1}{2a}\right) = 0$$

and obtain the solution for to the above quadratic equation for c_i is given by

$$c_i = \frac{-b_2 \pm \sqrt{b_2^2 - 4a\left(d_1 - \frac{b_1}{2a}\right)}}{2a} \qquad (5.22)$$

implying that we can have up to two possible values of c_i when we have $c_r = \frac{-d_2}{b_2} = \frac{-b_1}{2a}$. We shall denote this value of c_r as the critical c_r. These critical c_r

and c_i (shown later in section 5.4b) values are special as they are the values for which the equation (5.20) experiences a singularity.

5.4b Solution of c_i and implication on c_r

$$e_2 = 0 \Rightarrow 2ac_rc_i + b_2c_r + b_1c_i + d_2 = 0 \Rightarrow c_r = \frac{-b_1\left(c_i + \frac{d_2}{b_1}\right)}{2a\left(c_i + \frac{b_2}{2a}\right)}$$

Now, we substitute c_r, as shown above, into e_1 in (5.18) and we get:

$$ac_i^2 + b_2c_i - a\left(\frac{-b_1\left(c_i + \frac{d_2}{b_1}\right)}{2a\left(c_i + \frac{b_2}{2a}\right)}\right)^2 - b_1\left(\frac{-b_1\left(c_i + \frac{d_2}{b_1}\right)}{2a\left(c_i + \frac{b_2}{2a}\right)}\right) - d_1 = 0 \qquad (5.23)$$

As before, we seek to avoid the singularity and so convert (5.23) into a 4th order polynomial for c_i

$$\left(ac_i^2 + b_2c_i - d_1\right)(2ac_i + b_2)^2 - a(b_1c_i + d_2)^2 + b_1((b_1c_i + d_2))(2ac_i + b_2) = 0 \qquad (5.24)$$

As before, we want to investigate the "blow up" term, namely, $c_i = -\frac{b_2}{2a}$, which is defined to be one of the critical values of c_i.

When $c_i = -\frac{b_2}{2a}$, (5.24) becomes

$$-a\left(b_1\left(\frac{-b_2}{2a}\right) + d_2\right)^2 = 0 \Rightarrow \frac{d_2}{b_2} = \frac{b_1}{2a} \qquad (5.25)$$

which we immediately observe that (5.25) is similar to (5.21). Proceeding with the same analysis as in Section 5.4a, we now turn to (5.18) and substitute the relations into the complex component of (5.18), i.e. e_2, we obtain (5.25) again, as in Section 5.4a. Solving the real component of (5.18), i.e. e_1, for c_r, we subsequently obtain:

$$c_r = \frac{-b_1 \pm \sqrt{b_1^2 - 4a\left(d_1 - \frac{b_2}{2a}\right)}}{2a} \qquad (5.26)$$

Similarly, (5.26) implies that for this particular value of c_i, we can have up to two solutions for c_r.

5.4c Neutral Stability Condition

The definition of neutral stability means that the disturbance neither grows nor decays. Mathematically, the neutral stability criterion is expressed as $c_i = 0$ and using (5.18), we obtain $c_r = -\frac{d_2}{b_2}$ subject to $a\left(\frac{-d_2}{b_2}\right)^2 + b_1\left(\frac{-d_2}{b_2}\right) + d_1 = 0$. This latter condition is an additional constraint imposed to (5.21) or (5.25).

5.4d Format for General Solution for c_r and c_i

Turning to (5.20) and (5.24), we see a 4th order polynomial which means that there are 4 roots. Whether they are real or complex roots, it shall be determined in the computer program (D:/Thesis work/Chapter 5/main.m). We know from polynomial theory that there are four solution possibilities:

i. Four real roots.

ii. Two real roots and two complex conjugate roots.

iii. Four complex roots: two complex conjugate pairs.

Using the MAPLE programs (D:/Thesis Work/Chapter 5/solvecr.mws and D:/Thesis Work/Chapter 5/solveci.mws), the four roots of (5.20) and (5.24) will have the following analytical forms respectively:

$$c_r = \frac{-8ab_1 \pm 4\sqrt{2a^2b_1^2 - 8a^3d_1 - 2a^2b_2^2 \pm 2a^2\eta}}{16a^2} \tag{5.27}$$

$$c_i = \frac{-8ab_2 \pm 4\sqrt{2a^2b_2^2 + 8a^3d_1 - 2a^2b_1^2 \pm 2a^2\eta}}{16a^2} \tag{5.28}$$

where we have $\eta = \sqrt{16a^2d_1^2 - 8a\left(b_1^2 - b_2^2\right)d_1 + \left(b_1^2 + b_2^2\right)^2 + 16ad_2\left(ad_2 - b_1b_2\right)}$

We note that by the definition of c_r, we shall only take the real roots (observed to be taking the $+2a^2\eta$ term in the c_r and c_i expressions). We shall show why this is the case, using the SANTOS data, in Figure 2. We shall denote the positive discriminant as $2a^2b_2^2 + 8a^3d_1 - 2a^2b_1^2 + 2a^2\eta$ and $2a^2b_2^2 + 8a^3d_1 - 2a^2b_1^2 - 2a^2\eta$ as the negative

discriminant. The terms a, b_1, b_2, d_1 and d_2 are functions of interfacial height, H, mass flux of lower layer, ϕ, angle of inclination, α and wave number of the disturbance, γ.

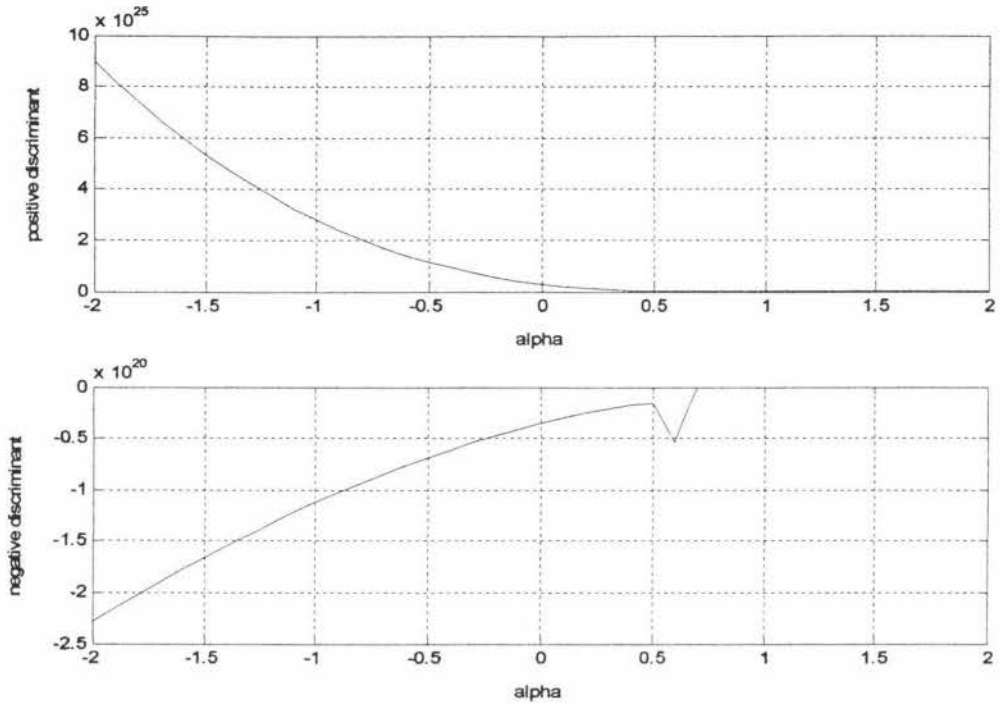

Figure 2 - Plot of positive and negative discriminants vs the angle of inclination, α

5.5 CASE STUDY - STABILITY OF BASE CASE

In this section, we shall look at some graphical output when we look at the base case, which employ the SANTOS data. We solve for c_i, using (5.28) and then substitute this value of c_i into $e_2 = 0$ (see (5.18)), to get c_r, noting that c_{i1} and c_{i2} correspond to taking the plus sign and minus sign in (5.28) respectively and that we are taking the positive discriminant. In addition, we have assigned wave numbers for the short perturbation wave and long perturbation wave scenario with $\gamma = 10^4$ and $\gamma = 10^{-4}$ respectively.

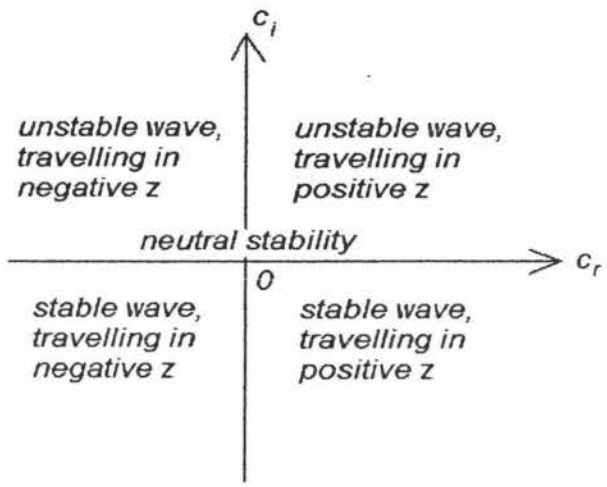

Figure 3 - Stability Map of the Possible Flow Scenario

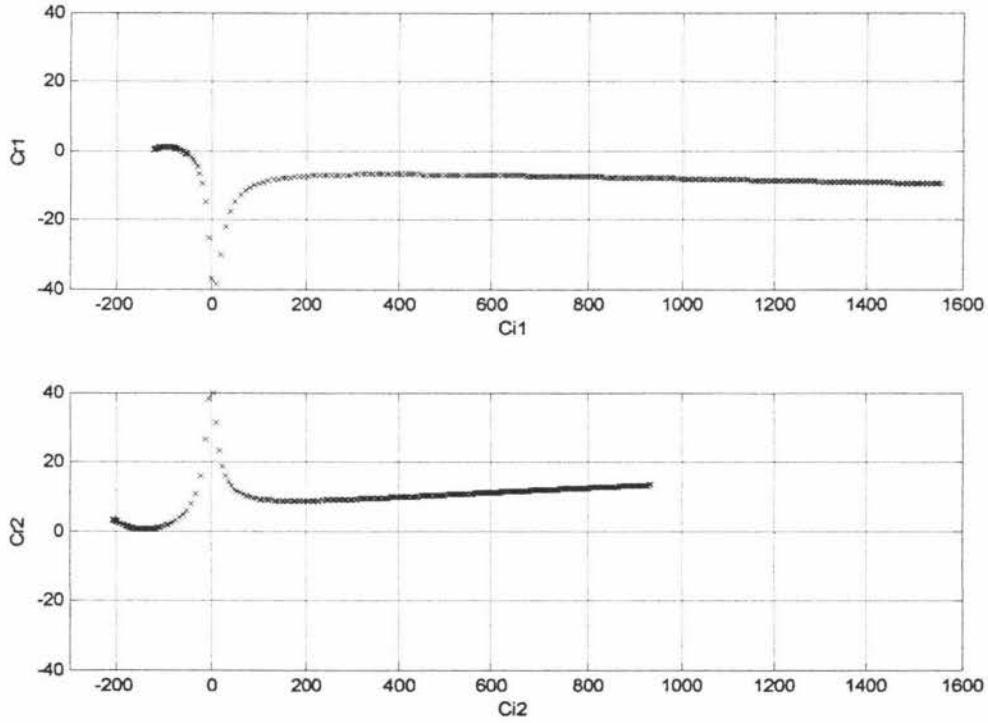

Figure 4a - Stability map of the Flow Scenario with long wave perturbations

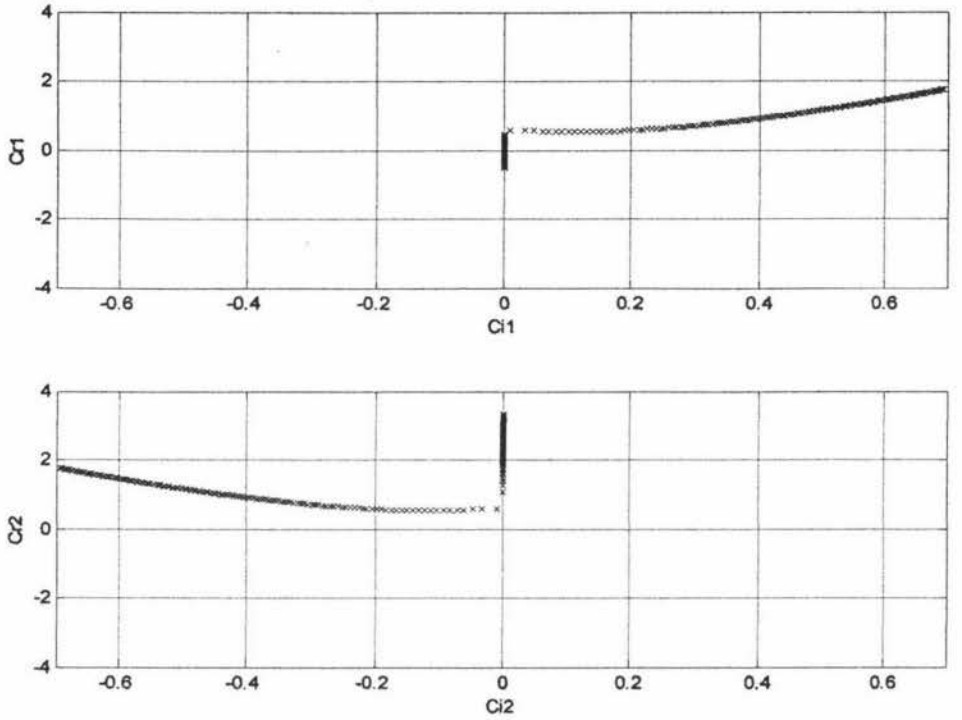

Figure 4b - Stability map of the Flow Scenario with short wave perturbations

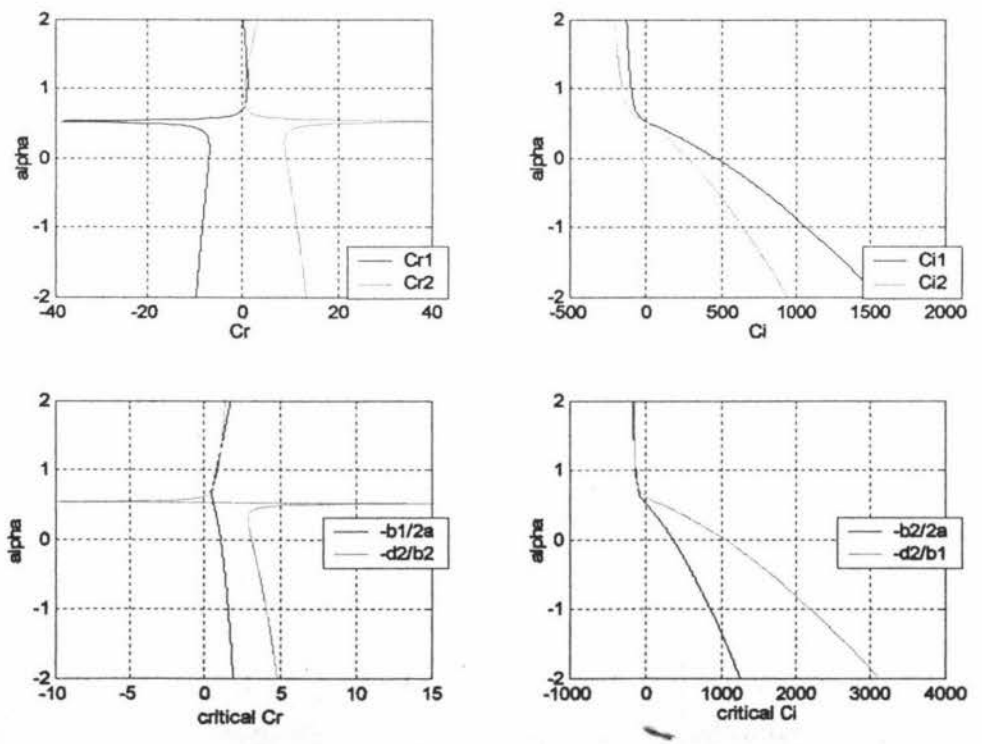

Figure 5a - Plots of α vs c_r, c_i and the critical values of c_r and c_i assuming long wave perturbation

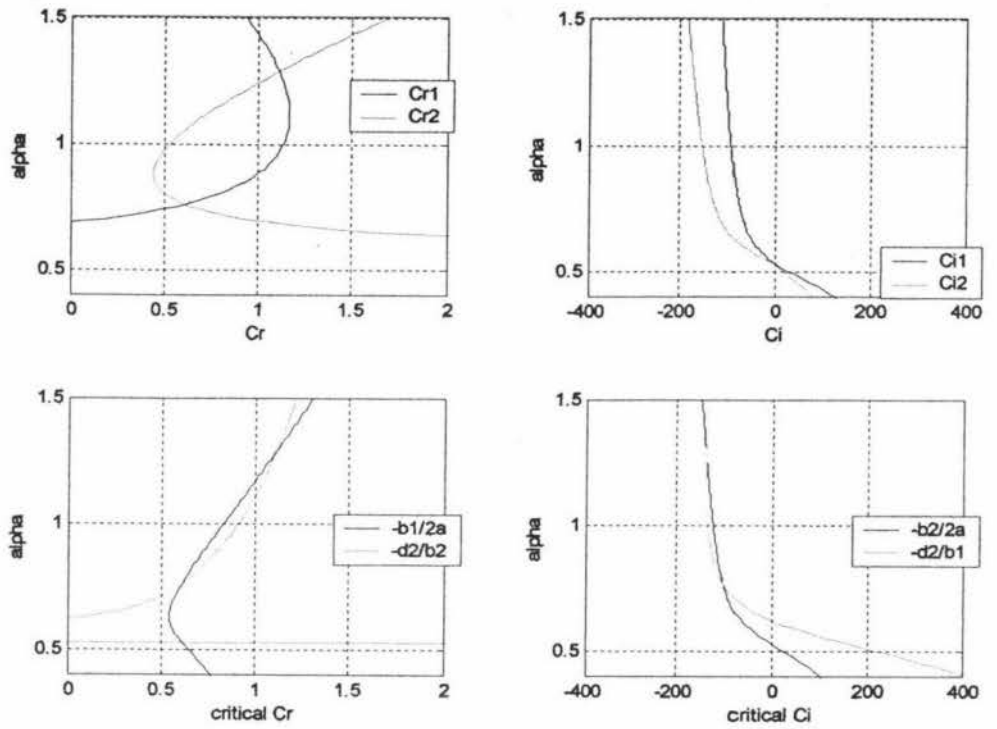

Figure 5b - Zoomed plots of α vs c_r, c_i and the critical values of c_r and c_i assuming long wave perturbation

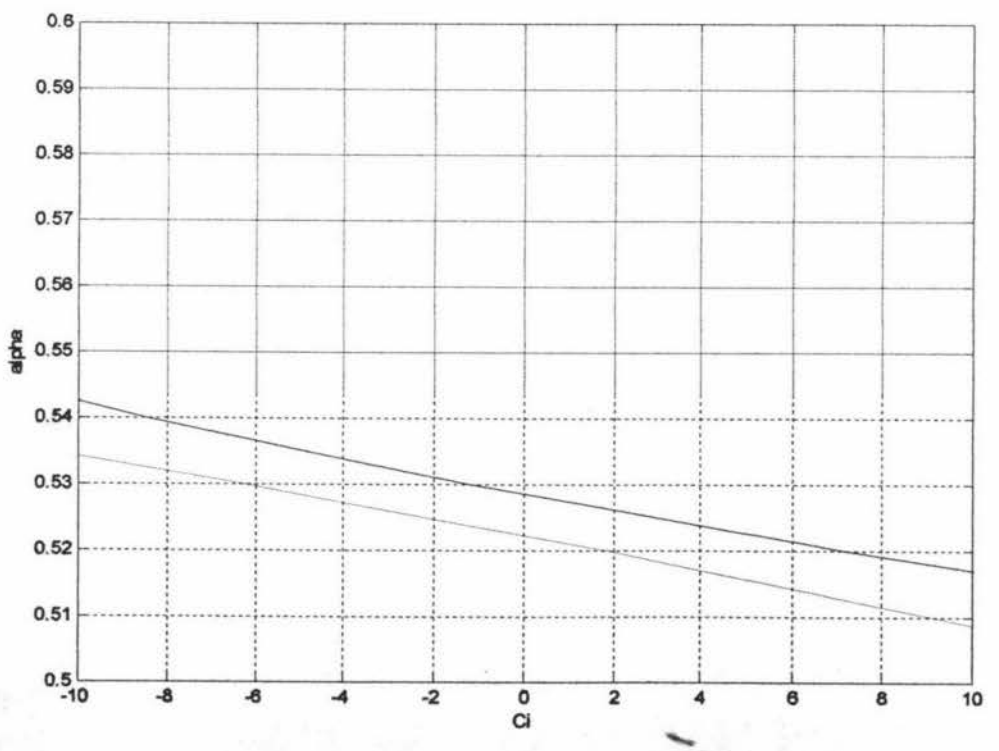

Figure 5c - Plots of α vs c_i with long wave perturbation

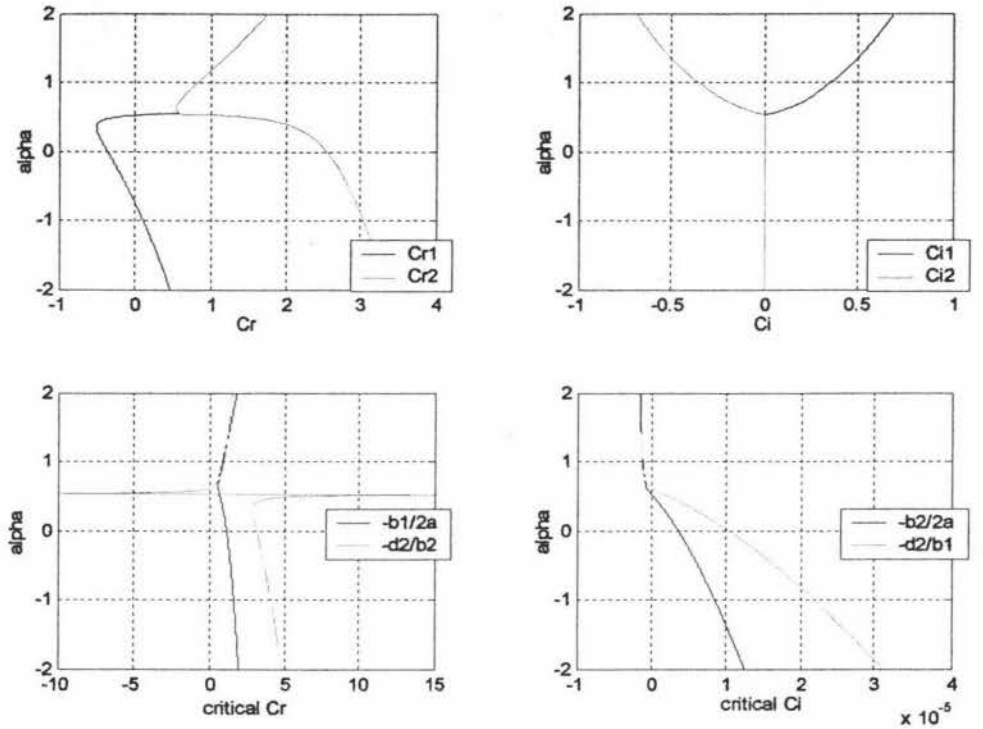

Figure 6a - Plots of α vs c_r, c_i and the critical values of c_r and c_i assuming short wave perturbations

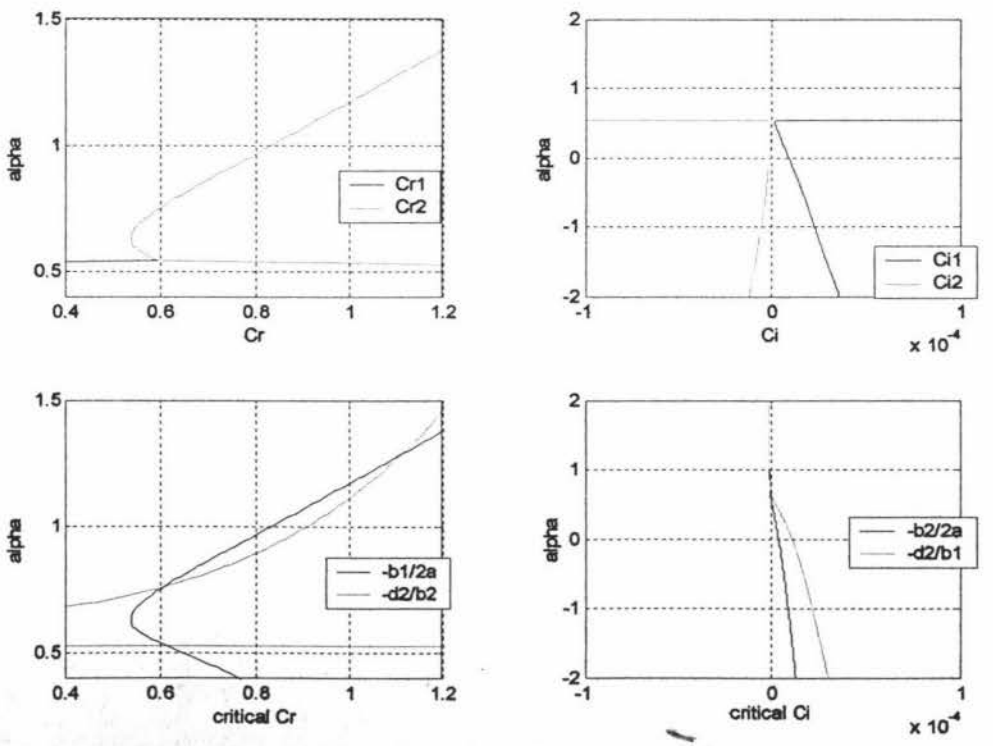

Figure 6b - Zoomed plots of α vs c_r, c_i and the critical values of c_r and c_i assuming short wave perturbations

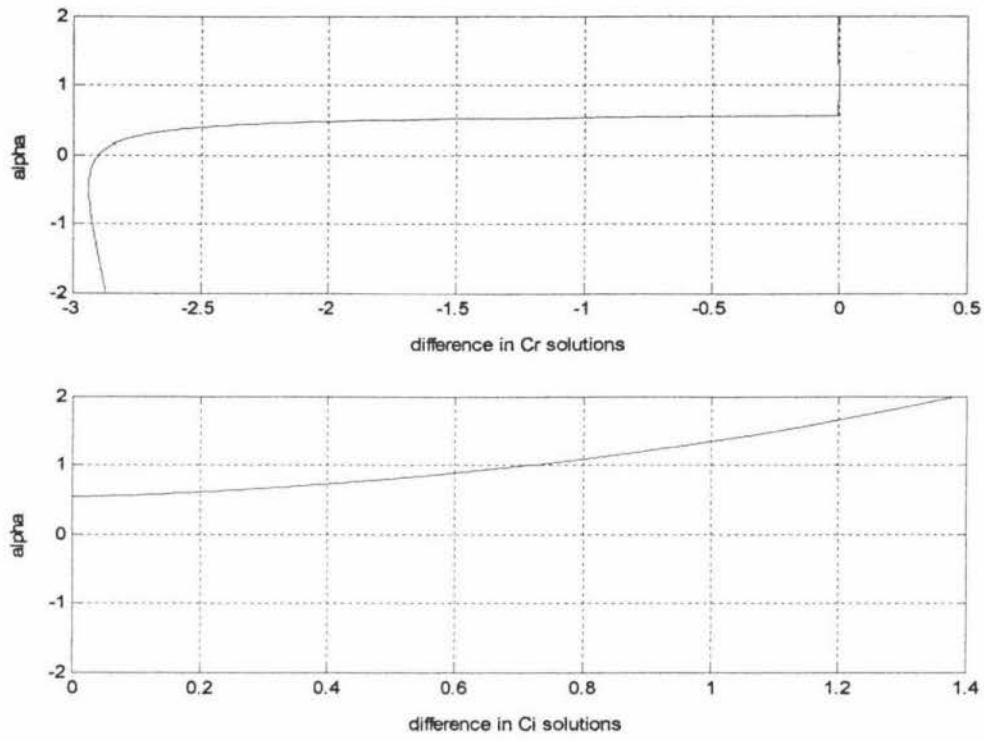

Figure 6c - Plots of α vs differences in c_r and c_i solutions assuming short wave perturbations

From the above plots (Figures 4-6), the following observations are made:

i. Assuming a long wave perturbation, the steady flow is mostly unstable (see Figure 4a) except for α approximately greater than and equal to 0.53 degrees.

ii. For long wave perturbations, the solution sets, (c_{r1}, c_{i1}) and (c_{r2}, c_{i2}) correspond to waves moving in downstream and upstream manner respectively (see Figure 4a).

iii. The first solution set (c_{r1}, c_{i1}) is unstable while the second solution set (c_{r2}, c_{i2}) is stable and moves downstream (see Figure 4b).

iv. For long wave perturbations, the two points that correspond to the intersection of c_{r1} and c_{r2} curves implies (5.25), as evident in the intersection of the critical c_{r1} and c_{r2} curves (See Figure 5a and 5b).

v. For long wave perturbations, we have no intersection of the c_{i1} and c_{i2} curves and their stability profile is similar, i.e. the c_{i1} and c_{i2} curves are not symmetric or anti-symmetric) (see Figure 5a and 5b).

vi. For short wave perturbations, the c_{i1} and c_{i2} solutions clearly correspond to the unstable and stable solutions respectively, with symmetry at $c_i = 0$ from the point

when the c_{r1} and c_{r2} curves intersect. (see Figure 6a and 6b). This is valid for $-1 \leq \alpha \leq 1$.

vii. The critical c_r curves are invariant with respect to the size of the wave number. This is evident in the terms featured in the analysis leading to (5.17) (see Figure 5a, 5b, 6a, 6b).

viii. (5.22) and (5.26) are supported as we see that for every c_r value, there are two c_i values and similarly, each c_i value corresponds to two c_r values.

5.6 Closing Remarks

Our final chapter of this thesis concludes with the stability of the steady state problem. We shall define the perturbation to be a travelling wave with a small amplitude (allowing us to linearize the resulting conservation relations) and determine if the perturbation grows (unstable) or decays (stable).

From the momentum conservation relation, we subsequently obtain the stability equation, which have real and complex terms. This stability equation yields two equations (e_1 and e_2) with two unknowns, namely the c_r (determines the direction of the travelling wave) and c_i (determines if the travelling wave grows or decays) terms. Our analysis was aimed at determining what happens as we vary the angle of inclination and assume short and long perturbation waves. The analysis was verified through the plots.

Chapter 6

CONCLUSION

6.1 SUMMARY OF RESULTS

Throughout this thesis, we have looked at possible scenarios involving the two-layered fluid system in a pipe. They are considered because of their physical significance and potential application. We have shown that despite the complexity of this problem, a lot of information has been discovered just by investigating this industrial problem using the three fundamental conservation relations.

In the introductory chapter (Chapter 1), we have demonstrated that the planar, cross-sectional interfacial configuration, as the model to describe the steady flow of a two-layered and stratified flow system in a circular pipeline, was valid. This was only possible when we had relatively low flow rates (volume flux) for both liquids and a high density differential between the two liquids are used. To simplify the problem, we have assumed that the two fluids have a high Reynolds number, allowing us to solve the speeds of the fluids by computing the averaged speeds, as determined by Equations (2.1a) and (2.1b).

In Chapter 2, the goal was to determine the relation between the interfacial height and the angle of inclination under the assumption that the average pressure gradients applied across both fluids are identical. It was stated that when this occurs, we have a uniform flow regime. This flow problem, and all the others, discussed in this thesis, were solved using the fundamental conservation relations of mass, momentum and energy. We showed that, when thermal effects are negligible, the momentum and energy conservation equations must yield similar results because there is no net energy flux loss or gain within the system (a single pipe section) under consideration. The energy conservation relation becomes relevant when we consider a pipe network consisting of multiple sections of varying angles of inclination or when we have a travelling pulse in a single section, the focus of Chapter 3.

Our travelling wave is assumed to have a short wavelength, which enables us to make further simplifications. Given the small axial length of such a wave, the dominant forces at play are the pressure force and the momentum flux changes across the wave. As with the setup in Chapter 2, we assumed that the flow regime behind and ahead of this travelling wave is uniform, i.e. the average pressure gradient in both these flow regions are equal. The significance of this is to see whether a short wave or a pulse induced can be sustained in a steady flow environment. We have showed that it can be sustained for angles of inclination greater than and equal to 0.5 degrees. For pipe section inclinations smaller than 0.5 degrees, we will not (subject to SANTOS flow data) have any travelling wave solution. We also presented 2 possible conceptual models where we assume that we

have a travelling pulse move from one pipe section to a different pipe section of a different angle of inclination.

We can add further complexity to Chapter 2 by considering the case when the axial interfacial pressure gradient varies slightly, as described in Chapter 4. As with Chapter 3, the energy flux relation tells us how much energy flux is lost in the pipe section(s).

Finally in Chapter 5, we want to see what happens when we perturb the steady state conditions slightly. The goal being that we want to see how stable is the flow system, i.e. how sensitive it is to slight disturbances to the steady fluid flows. We have also described how the various parameters of the flow system such as the angle of inclination, mass flux and the prospective wavelength of the disturbance have an effect on the stability of the flow regime.

6.2 FURTHER WORK

We have so far been looking at the case where we have the fluids moving in the axial pipeline direction. This is a feasible model by itself, given the SANTOS data which involved two liquids with a high relative density differential ($\Delta\rho/\rho_1 > 0.1$). To broaden the scope of the material for stratified flows, we could also consider cases where there is a low density differential between the two fluids ($\Delta\rho/\rho_1 \leq 0.1$) and significant thermal effects. In the first case (low density differential), surface tension and wetting effects become more important. So, there are three cases that would warrant further investigation.

First, we consider the varying cross-sectional interface, i.e. our interfacial function becomes $h(x,z)$. The difficulty with this model is that we now have to double the number of equations as we consider an additional dimension (x-direction). Due to the near infinite number of interfacial configurations (variation in the x-axis), it is also difficult to determine, in general terms, the terms in the equation depend on the x and z directions. The best course envisioned is to take data from industry and perform the analysis, as presented in this thesis.

Second, we factor the surface tension effects in the conservation relations. The surface tension term would turn the existing momentum and energy relations into a second order and nonlinear partial differential equation. Given the enormous complexity of the resulting equations and the numerous parameters involved, the best solution approach is a computational one.

So far, we have ignored the internal energy changes and described mechanical energy changes. To fully utilise the energy conservation relation, we also need to factor the heat losses due to the friction between the fluids and the fluids with the pipe walls. As we had shown in Chapter 4, the energy conservation equation yields the same relation as the momentum conservation relation. This is the third aspect that merits further investigation.

REFERENCES:

1. Isaacs, J.D., Speed, J.B, *U.S. Patent 759,374*, 1904.

2. Dussan, V.E.B, On the spreading of Liquids on Solid Surfaces: Static & Dynamic Contact Lines, *Annual Review of Fluid Mechanics*, Annual Reviews Inc, Palo Alto, vol. 11, p. 371, 1979.

3. Dussan, V.E.B., Davis, S.H., On the Motion of a Fluid-Fluid Interface Along a Solid Surface, *J. Fluid Mech.*, vol. 65, pp. 71-95, 1974.

4. Hasson, D., Mann, U., Nir, A., Annular Flow of Two Immiscible Liquids: I, Mechanisms, *Can. J. Chem. Engng.*, vol. 48, pp. 514-520, 1970.

5. Angeli, O., Hewitt, G. F., Pressure Drop Measurements in Oil and Water Prewetted pipes, *Int. Symp. on Liquid-Liquid Flow and Transport Phenomena*, Antayla, Turkey, 3-7 Nov. 1997.

6. Soleimani, A., Lawrence, C.J., Hewitt, G. F., Effect of Mixers on Flow Pattern and Pressure Drop in Horizontal Oil-Water Pipe Flow, *Int. Symp. on Liquid-Liquid Flow and Transport Phenomena*, Antayla, Turkey, 3-7 Nov. 1997.

7. Brauner, N., Liquid-Liquid Two Phase Flow, *The Update Journal of the Heat Exchanger Design Handbook,* Begell House Inc, pp. 1-32, 1998.

8. Oliemans, R.V.A., The Lubricating Film Model for Core-Annular Flow, *Ph.D. Thesis*, Delft University Press, 1986.

9. Oliemans, R.V.A., Ooms, G., Core-Annular Flow of Oil and Water Through a Pipeline, *Multiphase Science and Technology*, vol. 2, 1986.

10. Joseph, D. D., Renardy, Y. Y., *Fundamentals of Two Fluid Dynamics Parts I and II*, Springer-Verlag, 1992.

11. Brauner, N., Maron, D.M., Rovinsky, J., A Two-Fluid Model for Stratified Flows with Curved Interfaces, *Int. J. Multiphase Flow*, vol. 24, pp.975-1004, 1998.

12. Govier, G.W., Aziz, K., *The Complex Mixtures in Pipes*, Van Nostrand Reinhold Co, 1972.

13. Fozard, J. ,Terrain Slugging in Near Horizontal Oil Wells , *MSc thesis*, University of Oxford, 2001.

14. Brauner, N., Maron, D.M., Stability Analysis of Stratified Liquid-Liquid Flow, *Int. J. Multiphase Flow*, vol. 18, No.1, pp. 103-121, 1992.

15. McGuinness, M.J., McKibbin, R. Terrain-induced slugging. In: Hewitt, J. and Howlett, P. (eds) *Proceedings of the 2002 Mathematics-in-Industry Study Group held at the University of South Australia, Adelaide, Australia, 11-15 February, 2002*, MISG, 2003. In press.

16. Guo, L.J., Li, G.J and Chen, X.J., A Linear and Non-linear Analysis on Interfacial Instability of Gas-Liquid Two Phase Flow through a Circular Pipe, *Int. J. Multiphase Flow*, vol. 45, pp. 1525-1534, 2002.

BIBLIOGRAPHY

Acheson, D.J., *Elementary Fluid Dynamics*, Oxford University Press, 1998.

Andritsos, N., Hanratty, T.J., Interfacial Instabilities For Horizontal Gas-Liquid Flows in Pipelines, *Int. J. Multiphase Flow*, vol. 13, No. 5, pp. 583-603, 1987.

Barnea, D., Taitel, Y., Kelvin-Helmholtz Stability Criteria For Stratified Flow: Viscous versus Non-Viscous (Inviscid) Approaches, *Int. J. Multiphase Flow*, vol. 19, No. 4, pp. 639-649, 1993.

Benjamin, T.B., Internal Waves of finite amplitude and permanent form, *J. Fluid. Mech.*, vol. 25, No. 2, pp. 241-270,1966.

De Henau V., Raithby G. D., A Study of Terrain-Induced Slugging in Two-Phase Flow Pipelines, Intl J. Multiphase Flow, vol. 21, No 3, pp. 365-379, 1995.

De Henau V., Raithby G. D., A Transient Two-Fluid Model for The Simulation of Slug Flow in Pipelines – I. Theory, *Intl J. Multiphase Flow,* vol. 21, No 3, pp. 335-349, 1995.

De Henau V., Raithby G. D., A Transient Two-Fluid Model for The Simulation of Slug Flow in Pipelines – II. Validation, *Intl J. Multiphase Flow*, vol. 21, No 3, pp. 351-363, 1995.

Kowalski, J.E., Wall and Interfacial Shear Stress in Stratified Flow in Horizontal Pipe, *AIChE Journal*, Vol. 33, No. 2, pp. 274-281, 1987.

Lighthill, J., *Waves in Fluids*, Cambridge University Press, 1996.

McKibbin, R., Momentum and Energy Changes in the Flow of a Layered Liquid, Mathematical and Information Science Report (Massey University), Series B: 93/3, 1993.

Thorpe, S.A., Experiments on the Instability of Stratified Flows - Immiscible Fluids, *J. Fluid Mech.*, vol. 39, No. 3, pp. 25-48,1969.

Turner, J., *Buoyancy Effects in Fluids*, Cambridge University Press, 1979.

Wallis, G.B., *One Dimensional Two Phase Flow*, McGraw Hill, 1969.

Wood, I.R., Selective Withdrawal from a stably stratified fluid, *J. Fluid Mech.*, vol. 32, No. 2, pp. 209-223,1968.

Yih, C.S. and Guha, C.R., Hydraulic Jump in a Fluid System of Two Layers, *Tellus VII (3)*, 1955.